PLOS ONE

RESEARCH ARTICLE

KChIP2 genotype dependence of transient outward current (I_{to}) properties in cardiomyocytes isolated from male and female mice

Lara Waldschmidt, Vera Junkereit, Robert Bähring*

Institut für Zelluläre und Integrative Physiologie, Zentrum für Experimentelle Medizin, Universitätsklinikum Hamburg-Eppendorf, Hamburg, Germany

* r.baehring@uke.de

Citation: Waldschmidt L, Junkereit V, Bähring R (2017) KChIP2 genotype dependence of transient outward current (I_{to}) properties in cardiomyocytes isolated from male and female mice. PLoS ONE 12 (1): e0171213. doi:10.1371/journal.pone.0171213

Editor: Mark S. Shapiro, University of Texas Health Science Center, UNITED STATES

Received: November 1, 2016

Accepted: January 18, 2017

Published: January 31, 2017

Data Availability Statement: All relevant data are within the paper and its Supporting Information files.

Funding: This study was supported by grant BA2055/3 of the Deutsche Forschungsgemeinschaft (DFG) to RB. The funder had no role in study design, data collection and analysis, decision to publish, or preparation of the manuscript.

Competing Interests: The authors have declared that no competing interests exist.

Abstract

The transient outward current (I_{to}) in cardiomyocytes is largely mediated by Kv4 channels associated with Kv Channel Interacting Protein 2 (KChIP2). A knockout model has documented the critical role of KChIP2 in I_{to} expression. The present study was conducted to characterize in both sexes the dependence of I_{to} properties, including current magnitude, inactivation kinetics, recovery from inactivation and voltage dependence of inactivation, on the number of functional KChIP2 alleles. For this purpose we performed whole-cell patch-clamp experiments on isolated left ventricular cardiomyocytes from male and female mice which had different KChIP2 genotypes; i.e., wild-type ($KChIP2^{+/+}$), heterozygous knockout ($KChIP2^{+/-}$) or complete knockout of KChIP2 ($KChIP2^{-/-}$). We found in both sexes a KChIP2 gene dosage effect (i.e., a proportionality between number of alleles and phenotype) on I_{to} magnitude, however, concerning other I_{to} properties, $KChIP2^{+/-}$ resembled $KChIP2^{+/+}$. Only in the total absence of KChIP2 ($KChIP2^{-/-}$) we observed a slowing of I_{to} kinetics, a slowing of recovery from inactivation and a negative shift of a portion of the voltage dependence of inactivation. In a minor fraction of $KChIP2^{-/-}$ myocytes I_{to} was completely lost. The distinct KChIP2 genotype dependences of I_{to} magnitude and inactivation kinetics, respectively, seen in cardiomyocytes were reproduced with two-electrode voltage-clamp experiments on *Xenopus* oocytes expressing Kv4.2 and different amounts of KChIP2. Our results corroborate the critical role of KChIP2 in controlling I_{to} properties. They demonstrate that the Kv4.2/KChIP2 interaction in cardiomyocytes is highly dynamic, with a clear KChIP2 gene dosage effect on Kv4 channel surface expression but not on inactivation gating.

Introduction

A transient outward current (I_{to}) causes the initial (phase 1) repolarization of the action potential in ventricular cardiomyocytes [1], thereby controlling Ca^{2+} entry and excitation-contraction coupling [2]. A large portion of I_{to} is mediated by voltage-dependent K^+ (Kv) channels

belonging to the Kv4 subfamily [3–7] associated with cytoplasmic Kv Channel Interacting Proteins (KChIPs; [6, 8, 9]). Different genes are coding for Kv4.1, Kv4.2 and Kv4.3 channel subtypes, respectively, with two splice variants of Kv4.3 [10]. There are also different KChIP genes coding for KChIP1, KChIP2, KChIP3 and KChIP4, respectively, with different splice variants for each gene [11, 12]. The molecular correlates of I_{to} expression in cardiomyocytes have been extensively studied in several species (reviewed in [13]). Generally, there is abundant Kv4.2 and/or Kv4.3 expression and abundant KChIP2 expression, with different relative amounts depending on species, cardiac tissue and transmural cell layer [13].

Heterologous coexpression of Kv4 channels with KChIPs has been shown to modulate both channel expression and gating [8, 14, 15]. Binding of KChIPs increases Kv4 channel surface expression by various mechanisms, including promoted tetrameric assembly, a chaperone-like effect on trafficking, increased protein stability and promoted surface retention, all leading to a tremendous increase in measured current amplitudes [8, 14, 16–19]. Furthermore, KChIP binding modulates Kv4 channel inactivation properties, resulting in a slowing of macroscopic inactivation, an acceleration of recovery from inactivation and a positive shift in the voltage dependence of inactivation [8, 14, 15].

Two findings have initially led to the conclusion that KChIP2 plays an essential role in I_{to} expression in cardiomyocytes: The first finding has to do with the transmural I_{to} gradient observed in the ventricular free wall in many species, with larger I_{to} amplitudes usually found in epicardial than in endocardial myocytes [13]. This gradient has been reported to correlate with KChIP2 rather than Kv4 mRNA expression in humans and dogs [20]. The second finding concerns the I_{to} amplitudes measured in ventricular myocytes isolated from KChIP2 knockout mice [9]. I_{to} has been reported to be completely absent in myocytes of homozygous ($KChIP2^{-/-}$) and reduced by approximately half in myocytes of heterozygous ($KChIP2^{+/-}$) knockout mice. The latter finding was considered a possible KChIP2 gene dosage effect on I_{to} expression [9]; i.e., there seemed to be a proportionality between the number of functional KChIP2 alleles and the phenotypic I_{to} expression. However, the putative KChIP2 gene dosage effect has not been studied further and its applicability to the kinetics and voltage dependence of inactivation as well as its gender dependence have not been examined. The present study was conducted to characterize the KChIP2 genotype dependence of I_{to} properties in more detail. Using the same KChIP2 knockout mouse line we set out to answer the following questions related to the KChIP2 dependence of I_{to}: First, do all I_{to} properties show a KChIP2 gene dosage effect? Second, is there an absolute requirement of KChIP2 for the expression of I_{to}? And third, are there gender-dependent differences regarding the role of KChIP2 in the control of I_{to} properties? Our results confirm that KChIP2 is a key regulator of I_{to} in both sexes. However, I_{to} is not completely lost in the majority of homozygous KChIP2 knockout myocytes but kinetically modified. Our results reveal a partial KChIP2 gene dosage effect on I_{to}, because it is restricted to current magnitude.

Materials and methods

Ethical approval of animal procedures

This study was carried out in strict accordance with the local institutional guidelines after approval from local authorities (Institutional Animal Care and Use Committee: Behörde für Gesundheit und Verbraucherschutz, Hamburg, Germany; permit numbers: ORG349 and G119/15). Mice were sacrificed under isoflurane anesthesia, and frog surgery was performed under 3-aminobenzoate methanesulfonate anesthesia, and all efforts were made to minimize suffering.

Mouse line and cardiomyocyte preparation

Wild-type and genetically modified C57BL/6 mice (10–12 weeks old) were used for cardiomyocyte preparation. Genetically modified mice carried a heterozygous (+/-) or a homozygous deletion (-/-) of the KChIP2 gene. The generation and reactivation of the KChIP2 knockout mouse line have been previously described [9, 21]. For our experiments the animals were obtained from the local animal facility, where they were held at room temperature (20–22˚C), with food and water available *ad libitum*, and where they showed normal breeding. Genotyping was done based on tail biopsy. Mice were sacrificed by cervical dislocation under isoflurane anesthesia. The heart was excised, mounted on a temperature-controlled (37˚C) Langendorff perfusion system and rinsed with a Ca^{2+}-free solution (113 mM NaCl, 4.7 mM KCl, 0.6 mM KH_2PO_4, 0.6 mM Na_2HPO_4, 1.2 mM $MgSO_4$, 12 mM $NaHCO_3$, 10 mM $KHCO_3$, 30 mM taurine, 5.5 mM glucose, 10 mM HEPES, pH 7.46). Then the heart was digested for 9–10 min with the same solution containing 0.1 mg/ml Liberase Blendzyme (Roche). Epicardial tissue was obtained from the left ventricular free wall and dissociated into single cells. Ca^{2+} was stepwise reintroduced to a final concentration of 0.5–1 mM.

Patch-clamp recordings

Whole-cell patch-clamp recordings were performed on individual myocytes at room temperature (20–22˚C). The myocytes were bathed in extracellular solution containing 138 mM NaCl, 4 mM KCl, 1 mM $CaCl_2$, 2 mM $MgCl_2$, 0.33 NaH_2PO_4, 10 mM HEPES and 10 mM glucose (pH 7.3, NaOH). Patch pipettes were filled with internal solution containing 120 mM L-glutamate, 10 mM KCl, 2 mM K_2-ATP, 2 mM $MgCl_2$, 10 mM EGTA and 10 mM HEPES (pH 7.2, KOH). Recordings were done with an EPC-9 patch-clamp amplifier controlled by Pulse software (HEKA,). Pipette-to-bath resistance was between 2 and 2.5 MΩ, and the liquid junction potential (13 mV) was corrected online. Myocytes were held at -80 mV and outward currents were activated by depolarizing test pulses of different length to +40 mV. Series resistance (usually between 3 and 5 MΩ) was maximally compensated (70–80%). In order to inactivate a fraction of the currents conditioning prepulses were applied before the test pulse. Recovery from inactivation was studied with a double-pulse protocol (long control pulse and brief test pulse separated by an interpulse interval of different length at -80 mV). The voltage dependence of inactivation was studied with a variable prepulse protocol (long conditioning prepulse to different voltages between -100 and 0 mV followed by a brief test pulse).

Xenopus oocyte preparation and RNA injection

Kv4.2 channels were coexpressed in *Xenopus* oocytes with different amounts of KChIP2. *Xenopus* frogs were obtained from Nasco (Fort Atkinson, WI). The oocytes were surgically obtained under temporary ethyl 3-aminobenzoate methanesulfonate anesthesia. For this purpose 1.2 g of the anesthetic were disolved in 1 liter tap water together with 25 ml of a 0.5 M Na_2HPO_4 solution to keep the pH in a neutral range [22]. After surgical removal the oocytes were treated with collagenase for 3–4 h. After 12 h or later 50 nl of an aqueous cRNA solution were injected into individual oocytes with a Nanoliter 2000 microinjector (World Precision Instruments). The amount of Kv4.2 cRNA was always 1 ng per oocyte, whereas the amount of KChIP2 cRNA was varied between 0 and 12.8 ng per oocyte.

Two-electrode voltage-clamp recordings

Two-electrode voltage-clamp recordings from individual oocytes expressing Kv4.2/KChIP2 channels were done at room temperature (20–22˚C) between 24 h and 96 h after cRNA

injection. Voltage-clamp was achieved with a TurboTec-03 amplifier (npi) controlled by Pulse software (HEKA). Microelectrodes were filled with 3 M KCl and the oocytes were bathed in a solution containing 91 mM NaCl, 2 mM KCl, 1.8 mM $CaCl_2$, 1 mM $MgCl_2$ and 5 mM HEPES (pH 7.4, NaOH). Oocytes were held at -80 mV, and currents were activated by voltage pulses to +40 mV. The recovery from inactivation at -80 mV was studied with a double-pulse protocol.

Data analysis

Acquired current traces were analysed with Pulsefit (HEKA), and further data analysis and statistical tests were done with Kaleidagraph (Synergy Software). Current traces with a monophasic rapid decay, assigned to I_{to}, were generated with the prepulse-inactivation-subtraction method applied to cardiomyocytes ([23]; prepulse voltage -40 mV, prepulse duration 160 ms; see Fig 1A and S1 Fig). The decay of these current traces was fitted with a single-exponential function. The decay of compound outward currents obtained with 5 s long depolarizing pulses was fitted with a double- or a triple-exponential function. Root mean square (RMS) values in pA were used as a measure of fit accuracy. For each time constant (τx) an absolute amplitude (Ax) was provided by the fit. In our myocyte recordings τ1 and A1 obtained by triple-exponential fitting were assigned to I_{to}. We calculated relative amplitudes (relAx) in %, and, based on the whole-cell capacitance (Cap), current densities (Dx) in pA/pF (Dx = Ax / Cap). Based on $\sum_{X=2}^{3} Ax$(double-expoential fit) or $\sum_{X=1}^{3} Ax$ (triple-exponential fit), plus a leak corrected non-inactivating current component A0 (P/n method), we also calculated the total amplitude (AΣ) and density (DΣ) of the compound outward current. Both recovery from inactivation and the voltage dependence of inactivation were analyzed for the compound outward current neglecting A0 and leak current. Recovery kinetics were analyzed by fitting the data with a single- or a double-exponential function. Inactivation curves were obtained by fitting the data with a single or the sum of two Boltzmann-functions. Data are presented as mean ± SEM. Statistical significance between two groups was calculated by Student's *t*-test. For multiple comparisons, one-way analysis of variance (ANOVA) with Tukey's post-hoc test was performed. Differences with $p < 0.05$ were considered statistically significant. The concomitance of significant differences between $KChIP2^{+/+}$ and $KChIP2^{+/-}$, and between $KChIP2^{+/-}$ and $KChIP2^{-/-}$ (subject to a proportionality between the number of functional KChIP2 alleles and the phenotypic value) is referred to as a KChIP2 gene dosage effect on a given parameter.

Results

Isolation of I_{to}

The present study was performed to characterize in detail a possible KChIP2 gene dosage effect on I_{to} properties and its gender dependence. I_{to} properties included current magnitude (i.e., amplitude and density), decay and recovery kinetics and the voltage dependence of inactivation. We studied individual myocytes isolated from epicardial tissue of the left ventricular free wall from male and female mice with different KChIP2 genotypes; i.e., $KChIP2^{+/+}$, $KChIP2^{+/-}$ and $KChIP2^{-/-}$. For the detection of KChIP2 genotype- and/or gender-dependent differences a method both reliable and sensitive was needed for the isolation of I_{to}. Initially we applied both the prepulse-inactivation-subtraction method [23] and a method based on the analysis of the initial decay component derived from multi-exponential fitting of the compound outward current ([24–26]; see Materials and Methods). Fig 1 demonstrates the complementary application of the two methods to male $KChIP2^{+/+}$ myocytes. The prepulse-inactivation-subtraction method (Fig 1A, see also S1 Fig) yielded rapidly inactivating current traces, assigned to I_{to} at

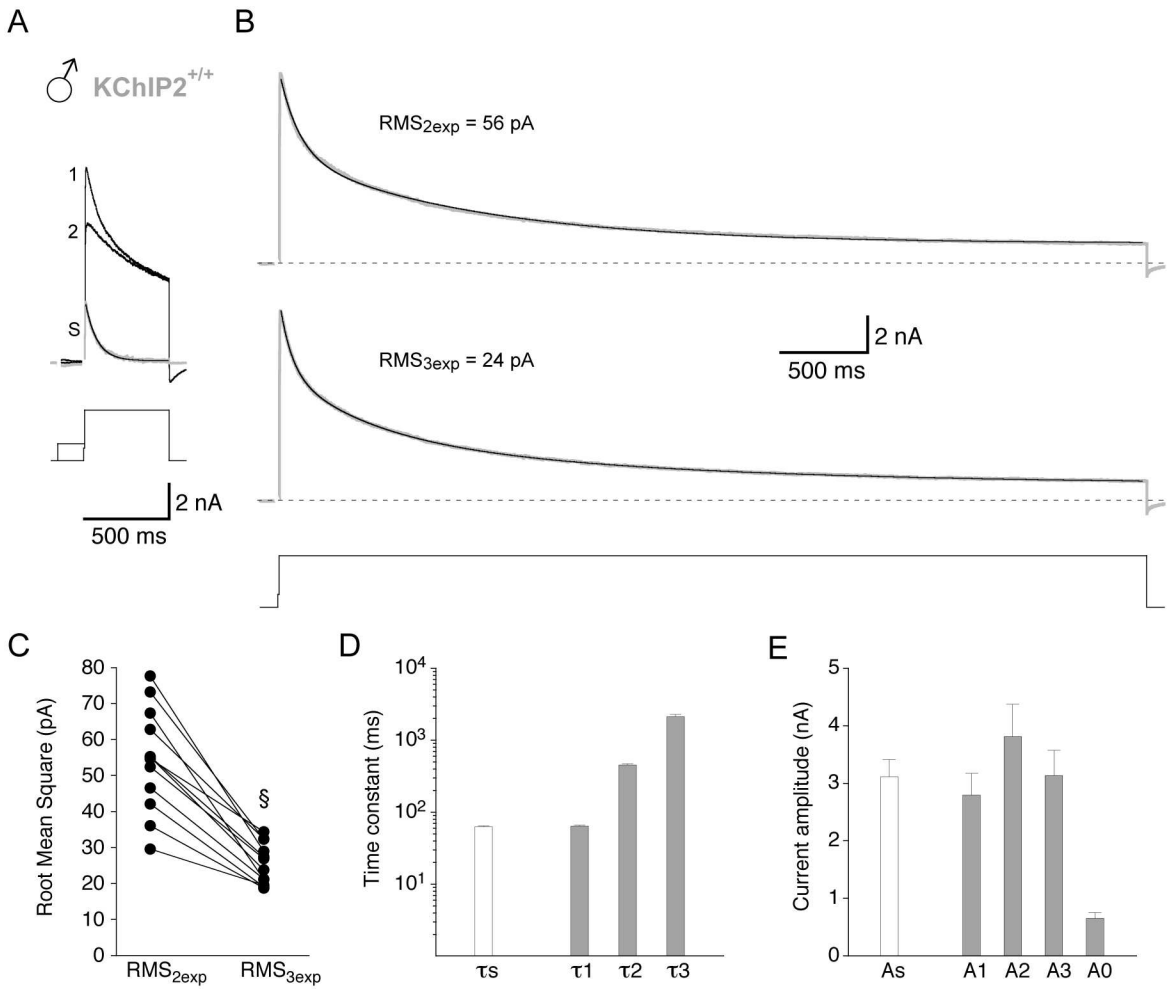

Fig 1. Isolation of I_{to} amplitude and inactivation kinetics. Whole-cell patch-clamp recordings were taken from individual murine cardiomyocytes isolated from the left ventricular free wall. Outward currents were activated by depolarizing voltage pulses from -80 to +40 mV. Inward sodium currents (not shown) were inactivated by a brief (8 ms) prepulse to -50 mV. Voltage protocols are shown below current traces. **A.** Prepulse-inactivation-subtraction method to isolate I_{to} in a male wild-type ($KChIP2^{+/+}$) myocyte. A fraction of current was optionally inactivated by a 160 ms prepulse to -40 mV. Subtraction of the remaining outward current (2) from the compound outward current (obtained without the 160 ms prepulse, 1) yielded a rapidly inactivating current trace (S), referred to as I_{to}. The inactivation of the I_{to} trace was fitted by a single-exponential function. **B.** Compound outward current recorded from the same myocyte as in A during a 5 s voltage pulse to +40 mV (dotted lines represent zero current). For the same current trace the decay was fitted by a double-exponential (2exp, top) and a triple-exponential function (3exp, bottom). The root mean square (RMS) values of the fits are indicated. **C.** Corresponding RMS_{2exp} and RMS_{3exp} values obtained for 12 male $KChIP2^{+/+}$ myocytes. RMS_{3exp} values were significantly smaller than RMS_{2exp} values (§, Student's paired *t*-test); i.e. the triple-exponential fit was more accurate. **D.** Mean time constants obtained by fitting the decay of isolated I_{to} traces with a single-exponential function (τs, empty bar) and by fitting the compound outward current decay with a triple-exponential function (τ1, τ2 and τ3, grey bars). Note the close match between τs and τ1. **E.** Mean peak amplitude of the isolated I_{to} traces (empty bar) and amplitudes of the individual time constants obtained by triple-exponential fitting (A1, A2 and A3, grey bars). The amplitude of the non-inactivating current component (A0, right grey bar) was obtained by fitting P/n leak-subtracted current traces (not shown).

doi:10.1371/journal.pone.0171213.g001

+40 mV, with a mean peak amplitude (As) of 3.11 ± 0.30 nA (n = 12; Fig 1E). Single-exponential fitting of these traces yielded a mean time constant of inactivation (τs) of 62.2 ± 2.1 ms (n = 12; Fig 1D). We also applied 5 s voltage pulses to +40 mV and fitted the decay of the compound outward currents with a double- and a triple-exponential function (Fig 1B). The triple-exponential function yielded better fits than the double-exponential function (RMS_{2exp} = 54.4 ± 4.2 pA,

RMS_{3exp} = 25.5 ± 1.6 pA, n = 12, $p<0.0001$, Student's paired *t*-test; Fig 1B and 1C). The time constants obtained with triple-exponential fitting were τ1 = 63.5 ± 2.4 ms, τ2 = 449 ± 19 ms and τ3 = 2107 ± 158 ms (n = 12). Notably, the time constant of the fastest decay component (τ1) was virtually identical to the one obtained with the prepulse-inactivation-subtraction method (τs; Fig 1D). Based on this finding and the higher fit accuracy we decided to use triple-exponential fitting, whenever appropriate, for our further analyses of compound outward current decay kinetics in cardiomyocytes. Accordingly, the time constant τ1 and its amplitude A1 from the triple-exponential fits were assigned to I_{to}. Similar to τ1 the I_{to} amplitude determined with triple-exponential fitting (A1 = 2.79 ± 0.38, n = 12) was very similar to the one obtained with the prepulse-inactivation-subtraction method (As; Fig 1E; no statistical test performed). The fit results (mean time constants and amplitudes) for male myocytes are summarized in Table 1, together with mean RMS values (in pA) for the double- and triple-exponential fits, relative amplitudes of the individual time constants (relAx) in %, whole-cell capacitance (Cap) in pF and current densities (Dx) in pA/pF, as well as the total amplitude and density (AΣ and DΣ, respectively) of the compound outward current at +40 mV. Taken together, comparable to the prepulse-inactivation-subtraction results (see S1 Table), triple-exponential fitting yielded an I_{to} amplitude of ~3 nA with an inactivation time constant of ~60 ms in male $KChIP2^{+/+}$ myocytes. The absolute amplitudes and densities of the fast (I_{to}-related), the intermediate and the slow component, as well as their relative contributions to the compound outward current decay (30%, 38% and 32%, respectively) were more or less balanced. The non-inactivating current component A0 was smaller than A1, A2 and A3 (see Fig 1E and Table 1).

KChIP2 genotype dependence of I_{to} properties in male myocytes

Fig 2A shows the inactivating components of normalized current traces obtained with a 5 s voltage pulse to +40 mV from male myocytes which had different KChIP2 genotypes. Currents from wild-type ($KChIP2^{+/+}$) myocytes showed the fastest decay kinetics, whereas currents from heterozygous ($KChIP2^{+/-}$) and homozygous KChIP2 knockout myocytes ($KChIP2^{-/-}$) decayed more slowly. Notably, in some $KChIP2^{-/-}$ myoctes (7 out of 26) current decay was extremely slow. Similar to $KChIP2^{+/+}$, outward current decay kinetics were best described by a triple-exponential function in all $KChIP2^{+/-}$ and most $KChIP2^{-/-}$ myocytes (19 out of 26). The fit results are shown in Fig 2B and 2C (see also Table 1). In $KChIP2^{+/-}$ myocytes the I_{to} kinetics (τ1 = 61.7 ± 3.0 ms, n = 38) were not significantly different from $KChIP2^{+/+}$, whereas $KChIP2^{-/-}$ I_{to} kinetics (τ1 = 81.7 ± 4.9 ms, n = 19) were slower. I_{to} amplitude, on the other hand, was smaller, compared to $KChIP2^{+/+}$, in $KChIP2^{+/-}$ myocytes (A1 = 1.77 ± 0.12 nA, n = 38) and even smaller in $KChIP2^{-/-}$ myocytes (A1 = 0.75 ± 0.11 nA, n = 19). Neither the intermediate nor the slow decay kinetics showed a dependence on the KChIP2 genotype (Fig 2B), however, A2 was reduced in a KChIP2 genotype-dependent manner, as was the amplitude of the non-inactivating current component A0 (Fig 2C). Accordingly, the total amplitude of the compound outward current (AΣ) was also reduced in a KChIP2 genotype-dependent manner (Fig 2D and Table 1). In the $KChIP2^{-/-}$ myocytes with an extremely slow current decay, the kinetics were well described by a double-exponential function (Fig 2A and Table 1). In these $KChIP2^{-/-}$ myocytes the time constants of the fast and slow decay component obtained with double-exponential fitting were virtually identical to the time constants of the intermediate and slow component obtained for all other myocytes with triple-exponential fitting (Fig 2B). However, their amplitudes appeared larger than the corresponding values obtained in the other $KChIP2^{-/-}$ myocytes (Fig 2C), and therefore, the total amplitude AΣ was comparable in all male $KChIP2^{-/-}$ myocytes (Fig 2D and Table 1; no statistical tests performed). Taken together, in male myocytes I_{to} amplitude showed a clear KChIP2 gene dosage effect, with a

Table 1. Data summary for male cardiomyocytes.

♂	KChIP2$^{+/+}$	KChIP2$^{+/-}$	KChIP2$^{-/-}$	
	3exp	3exp	3exp	*2exp*
RMS_{2exp} (pA)	54.4 ± 4.2	44.4 ± 2.2	25.8 ± 1.3	*25.9 ± 3.1*
RMS_{3exp} (pA)	25.5 ± 1.6 §	22.0 ± 0.8 §	20.0 ± 0.9 §	*21.2 ± 1.5*
Current kinetics and magnitudes				
τ1 (ms)	63.5 ± 2.4	61.7 ± 3.0	81.7 ± 4.9 **	-
τ2 (ms)	449 ± 19	436 ± 15	451 ± 26	*444 ± 29*
τ3 (ms)	2107 ± 158	2218 ± 115	2274 ± 177	*2154 ± 274*
A1 (nA)	2.79 ± 0.38	1.77 ± 0.12 *	0.75 ± 0.11 **	-
A2 (nA)	3.81 ± 0.56	3.00 ± 0.25	2.28 ± 0.27 *	*3.32 ± 0.53*
A3 (nA)	3.13 ± 0.44	2.42 ± 0.18	2.13 ± 0.21	*2.72 ± 0.32*
A0 (nA)	0.65 ± 0.10	0.25 ± 0.05 *	0.30 ± 0.06 *	*0.55 ± 0.11*
AΣ (nA)	10.4 ± 0.79	7.43 ± 0.43 *	5.46 ± 0.48 **	*6.59 ± 0.87*
relA1 (%)	30 ± 5	26 ± 2	16 ± 2 **	-
relA2 (%)	38 ± 4	40 ± 2	42 ± 2	*54 ± 3*
relA3 (%)	32 ± 3	34 ± 1	42 ± 2	*46 ± 3*
Cap (pF)	189 ± 12	169 ± 8	170 ± 13	*167 ± 6*
D1 (pA/pF)	15.6 ± 2.4	11.1 ± 0.8 *	4.9 ± 0.7 **	-
D2 (pA/pF)	20.3 ± 2.7	18.3 ± 1.5	14.2 ± 1.7	*19.7 ± 2.8*
D3 (pA/pF)	16.4 ± 1.9	14.4 ± 0.9	12.9 ± 0.9	*16.3 ± 1.7*
D0 (pA/pF)	3.4 ± 0.5	1.4 ± 0.3 *	2.0 ± 0.4	*3.2 ± 0.5*
DΣ (pA/pF)	55.6 ± 3.6	45.2 ± 2.3	34.0 ± 2.9 **	*39.2 ± 4.6*
	(n = 12)	(n = 38)	(n = 19)	*(n = 7)*
Recovery from inactivation				
$\tau_{rec}1$ (ms)	94.5 ± 5.4	88.6 ± 5.7	381 ± 43 **	*245 / 730*
$\tau_{rec}2$ (ms)	1490 ± 145	1210 ± 69	2296 ± 215 **	*1825 / 3736*
$A_{rec}1$ (%)	63 ± 2	56 ± 6	58 ± 2	*59 / 65*
$A_{rec}2$ (%)	37 ± 2	44 ± 2	42 ± 3	*41 / 35*
	(n = 9)	(n = 36)	(n = 11)	*(n = 2)*
Voltage dependence of inactivation				
$V_{1/2}1$ (mV)	-52.8 ± 1.4	-54.1 ± 0.8	-69.7 ± 5.4 **	-
$V_{1/2}2$ (mV)	-36.1 ± 3.5	-34.1 ± 0.9	-34.9 ± 1.4	*-33.0 ± 2.8*
A_V1 (%)	63 ± 8	52 ± 4	10 ± 1 **	-
A_V2 (%)	37 ± 8	48 ± 4	90 ± 1 **	-
	(n = 11)	(n = 31)	(n = 11)	*(n = 3)*

Analysis results obtained for current kinetics and magnitudes, recovery from inactivation and voltage dependence of inactivation for male myocytes with different KChIP2 genotypes.

* significantly different from KChIP2$^{+/+}$;

** significantly different from both KChIP2$^{+/+}$ and KChIP2$^{+/-}$ (one way ANOVA);

§ significantly different from RMS_{2exp} (paired Student's *t*-test); abbreviations are explained in the text.

doi:10.1371/journal.pone.0171213.t001

reduction from ~ 3 nA in KChIP2$^{+/+}$ to ~ 2 nA in KChIP2$^{+/-}$ and to ~ 1 nA in KChIP2$^{-/-}$. I_{to} density was equally affected since whole-cell capacitance (i.e., cell size) was not significantly different among KChIP2 genotypes (Table 1). In male KChIP2$^{-/-}$ myocytes I_{to} had an increased inactivation time constant (~80 ms), and I_{to} only accounted for 16% of the compound outward current decay, while either of the two remaining components accounted for 42% (Table 1). In a fraction of male KChIP2$^{-/-}$ myocytes I_{to} was apparently lost.

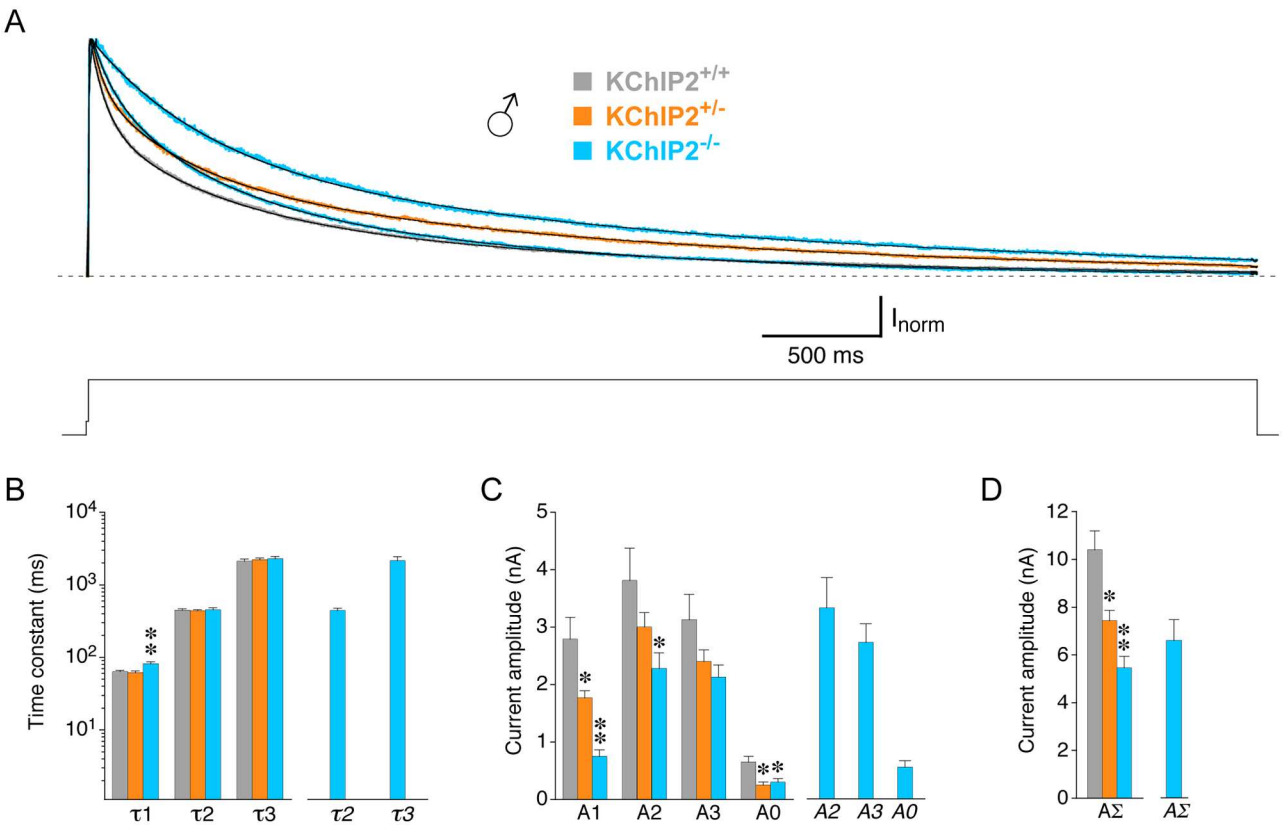

Fig 2. Multi-exponential fitting of compound outward current decay in male myocytes with different KChIP2 genotypes. Outward currents were activated by 5 s voltage pulses from -80 to +40 mV in male KChIP2$^{+/+}$, KChIP2$^{+/-}$ and KChIP2$^{-/-}$ myocytes. The voltage protocol is shown below the current traces. **A.** Representative current traces for the different KChIP2 genotypes were normalized to peak and only the inactivating current components are shown (dotted line represents non-inactivating current level). Current decay kinetics in KChIP2$^{+/+}$ (grey), KChIP2$^{+/-}$ (orange) and most KChIP2$^{-/-}$ myocytes (19 out of 26, blue, fast decay) were best described by a triple-exponential function. In some KChIP2$^{-/-}$ myocytes (7 out of 26, blue, slow decay) a double-exponential function was sufficient. **B.** Mean time constants (τ1, τ2 and τ3) obtained with a triple-exponential function for male KChIP2$^{+/+}$ (grey bars), KChIP2$^{+/-}$ (orange bars) and most KChIP2$^{-/-}$ myocytes (19 out of 26, blue bars), and mean time constants obtained with a double-exponential function for 7 out of 26 male KChIP2$^{-/-}$ myocytes (*τ2* and *τ3*, separate blue bars on the right). **C.** Mean amplitudes of the individual time constants obtained by triple-exponential (A1, A2 and A3) and double-exponential fitting (*A2* and *A3*, separate bars on the right), and mean amplitudes of the corresponding non-inactivating current components (A0, *A0*). Note the KChIP2 gene dosage effect on A1. **D.** Mean total amplitudes of the compound outward current (AΣ, *AΣ*). The KChIP2 gene dosage effect observed for A1 is also reflected in AΣ (* significantly different from KChIP2$^{+/+}$; ** significantly different from both KChIP2$^{+/+}$ and KChIP2$^{+/-}$; one-way ANOVA).

doi:10.1371/journal.pone.0171213.g002

Next we studied the recovery of the compound outward current from inactivation in male myocytes with a double-pulse protocol (Fig 3A; see Materials and Methods). For all three KChIP2 genotypes the recovery kinetics were best described by a double-exponential function (Fig 3B). In male myocytes KChIP2$^{+/+}$ and KChIP2$^{+/-}$ recovery kinetics were virtually identical (KChIP2$^{+/+}$: $\tau_{rec}1$ = 94.5 ± 5.4 ms, 63%; $\tau_{rec}2$ = 1490 ± 145 ms, 37%; n = 9; KChIP2$^{+/-}$: $\tau_{rec}1$ = 88.6 ± 5.7 ms, 56%; $\tau_{rec}2$ = 1210 ± 69 ms, 44%; n = 36; Fig 3B–3D). KChIP2$^{-/-}$ myocytes showed slower recovery kinetics due to larger recovery time constants with more or less unchanged relative contributions ($\tau_{rec}1$ = 381 ± 43 ms, 58%; $\tau_{rec}2$ = 2296 ± 215 ms, 42%; n = 11; Fig 3B and 3D and Table 1). The data obtained from two KChIP2$^{-/-}$ myocytes with an apparent loss of I_{to} suggested similar recovery kinetics in all male KChIP2$^{-/-}$ myocytes (Table 1).

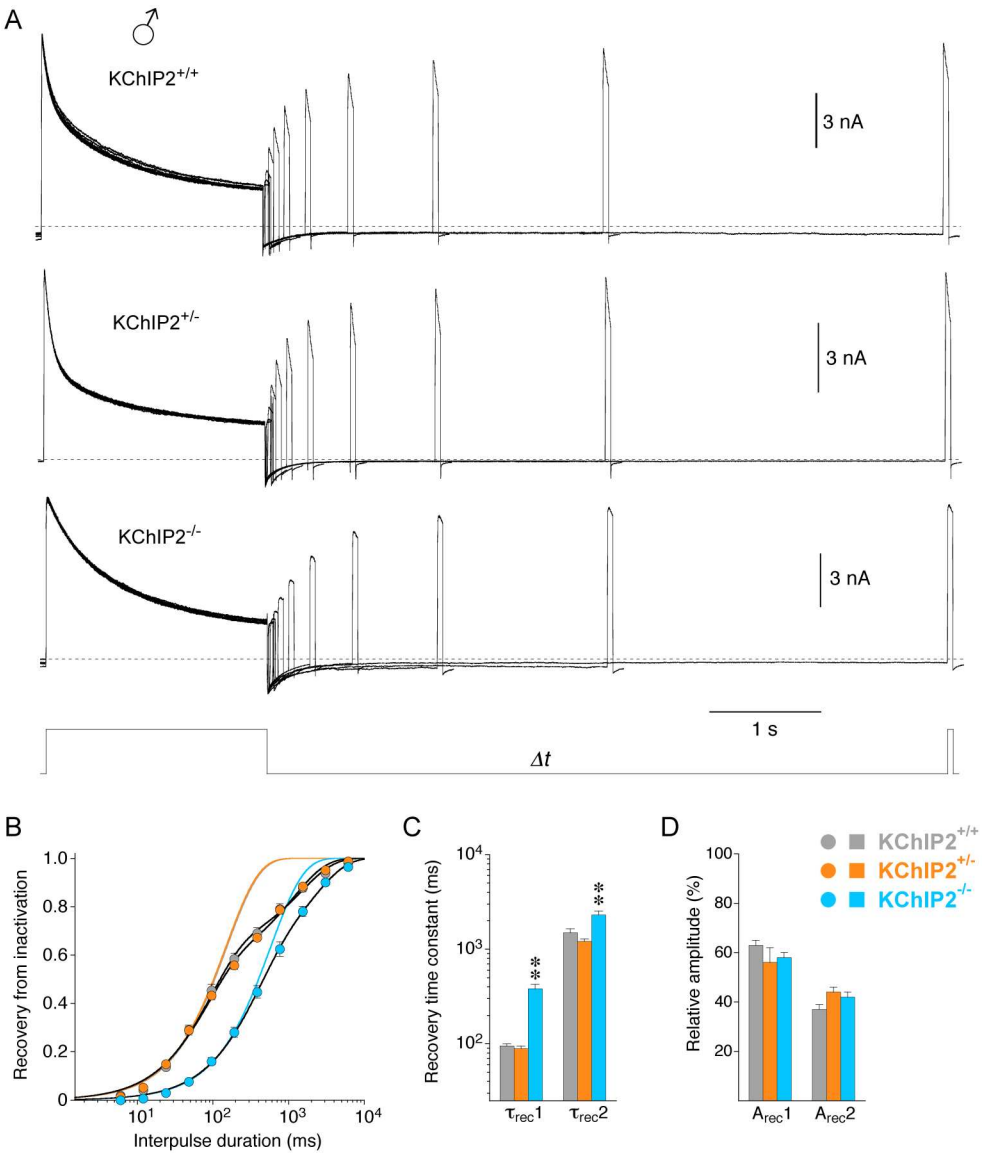

Fig 3. Recovery from inactivation in male myocytes with different KChIP2 genotypes. Recovery from inactivation at -80 mV was studied in male myocytes using a double-pulse protocol with interpulse durations between 6 ms and 6.14 s (*Δt*) followed by a brief test pulse (voltage protocol shown below current traces). **A.** Representative current families, recorded with the double-pulse protocol for the different KChIP2 genotypes (dotted lines represent zero current). **B.** Relative peak current amplitudes obtained with the brief test pulse were plotted against interpulse duration for the different KChIP2 genotypes ($KChIP2^{+/+}$: grey, $KChIP2^{+/-}$: orange, $KChIP2^{-/-}$: blue), and the data were fitted with a double-exponential function. Recovery kinetics for $KChIP2^{+/+}$ and $KChIP2^{+/-}$ were virtually identical. Lines without symbols represent single-exponential functions fitted to a fraction of the data points and forced to reach 1 (orange and grey line superimpose). They represent the fast recovery component and emphasize the necessity of a double-exponential function to adequately fit the recovery kinetics for all KChIP2 genotypes. **C.** Mean recovery time constants ($\tau_{rec}1$ and $\tau_{rec}2$) obtained by double-exponential fitting (** significantly different from both $KChIP2^{+/+}$ and $KChIP2^{+/-}$; one-way ANOVA). **D.** Mean relative amplitudes of the recovery time constants ($A_{rec}1$ and $A_{rec}2$).

doi:10.1371/journal.pone.0171213.g003

The voltage dependence of compound outward current inactivation of male myocytes was studied with a variable prepulse protocol (Fig 4A; see Materials and Methods). For all three KChIP2 genotypes the data were best described by the sum two Boltzmann-functions (Fig 4B), defining a first (more negative) and a second (less negative) component. Similar to the

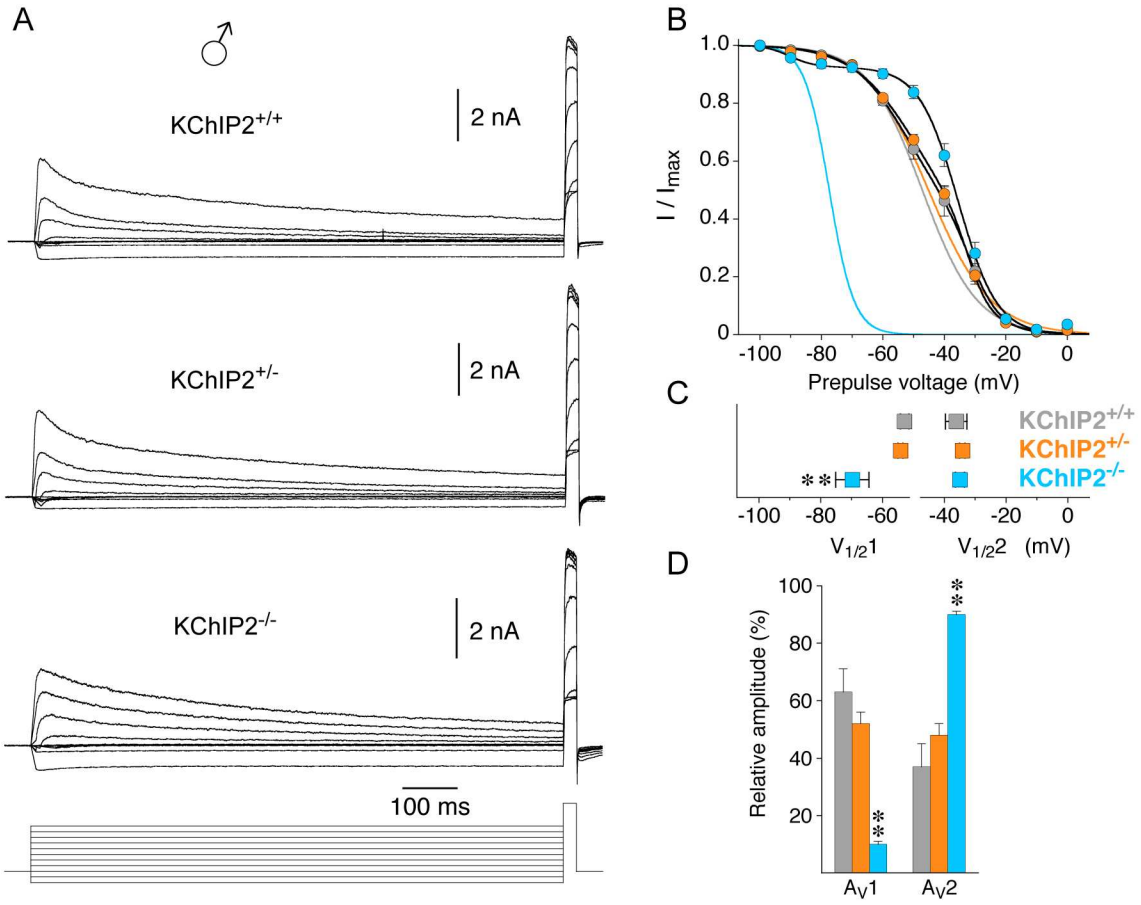

Fig 4. Voltage dependence of inactivation in male myocytes with different KChIP2 genotypes. The voltage dependence of inactivation was studied in male myocytes with a variable prepulse protocol. The prepulse (1 s, between -100 and 0 mV) was followed by a brief test pulse (voltage protocol shown below current traces). **A.** Representative current families, recorded with the variable prepulse protocol, for the different KChIP2 genotypes. **B.** Normalized peak current amplitudes obtained with the test pulse (I / I_{max}) were plotted against prepulse voltage for the different KChIP2 genotypes ($KChIP2^{+/+}$: grey, $KChIP2^{+/-}$: orange, $KChIP2^{-/-}$: blue), and the data were fitted with the sum of two Boltzmann-functions. The voltage dependences for $KChIP2^{+/+}$ and $KChIP2^{+/-}$ were virtually identical. Lines without symbols represent single Boltzmann-functions fitted to a fraction of the data points and forced to reach 0. They extrapolate the more negative portion of the voltage dependences and emphasize the necessity of the sum of two Boltzmann-functions to adequately fit the voltage dependence of inactivation. **C.** Mean values of the voltages of halfmaximal inactivation obtained for the two components ($V_{1/2}1$ and $V_{1/2}2$) obtained with the sum of two Boltzmann-functions. Note that $V_{1/2}1$ was shifted to more negative potentials for $KChIP2^{-/-}$, whereas $V_{1/2}2$ values were similar in all KChIP2 genotypes. **D.** Mean relative amplitudes of the two components defined by $V_{1/2}1$ and $V_{1/2}2$, respectively (A_v1 and A_v2); ** significantly different from both $KChIP2^{+/+}$ and $KChIP2^{+/-}$; one-way ANOVA).

doi:10.1371/journal.pone.0171213.g004

recovery kinetics, the voltage dependence of inactivation in male myocytes was almost identical for $KChIP2^{+/+}$ and $KChIP2^{+/-}$ ($KChIP2^{+/+}$: $V_{1/2}1$ = -52.8 ± 1.4 mV, 63%; $V_{1/2}2$ = -36.1 ± 3.5 mV, 37%; n = 11; $KChIP2^{+/-}$: $V_{1/2}1$ = -54.1 ± 0.8 mV, 52%; $V_{1/2}2$ = -34.1 ± 0.9 mV, 48%; n = 31; Fig 4B–4D). Intriguingly, male $KChIP2^{-/-}$ myocytes showed a negative shift in $V_{1/2}1$ (-69.7 ± 5.4 mV) with no change in $V_{1/2}2$ (-34.9 ± 1.4 mV, n = 11; Fig 4C), and the component defined by $V_{1/2}1$ only accounted for 10% (Fig 4D and Table 1). In the male $KChIP2^{-/-}$ myocytes with an apparent loss of I_{to} a single Boltzmann-function was sufficient to describe the voltage dependence of inactivation and the resultant $V_{1/2}$ value (-34.9 ± 1.4 mV, n = 3) resembled $V_{1/2}2$ obtained for all other myocytes with the sum of two Boltzmann-functions (Table 1).

I_{to} properties in female myocytes

In the present study I_{to} properties were also examined for female myocytes (summarized in Table 2). Before we will describe their KChIP2 genotype dependence we compare the I_{to} properties found in male and female KChIP2$^{+/+}$ myocytes. The data obtained from female myocytes displayed the same fit requirements. The triple-exponential fitting analysis method to isolate I_{to} from female myocytes (Fig 5A) yielded a time constant τ1 of 54.4 ± 2.3 ms (n = 16),

Table 2. Data summary for female cardiomyocytes.

♀	KChIP2$^{+/+}$	KChIP2$^{+/-}$	KChIP2$^{-/-}$	
	3exp	**3exp**	**3exp**	***2exp***
RMS_{2exp} (pA)	50.4 ± 5.0	43.4 ± 2.0	36.5 ± 3.1	*18.8 ± 3.8*
RMS_{3exp} (pA)	20.3 ± 1.2 §	20.3 ± 0.6 §	20.8 ± 1.1 §	*16.1 ± 2.1*
Current kinetics and magnitudes				
τ1 (ms)	54.4 ± 2.3 ¶	58.2 ± 1.3	70.3 ± 7.0 **	-
τ2 (ms)	436 ± 20	447 ± 10	442 ± 14	*241 ± 19*
τ3 (ms)	2544 ± 222	2654 ± 114	2399 ± 286	*2440 ± 367*
A1 (nA)	2.93 ± 0.33	1.94 ± 0.11 *	1.23 ± 0.15 **	-
A2 (nA)	2.72 ± 0.43	2.56 ± 0.19	2.87 ± 0.37	*0.74 ± 0.43*
A3 (nA)	1.83 ± 0.19 ¶	1.99 ± 0.09	1.96 ± 0.13	*1.99 ± 0.25*
A0 (nA)	0.28 ± 0.07 ¶	0.24 ± 0.03	0.38 ± 0.07	*0.16 ± 0.09*
AΣ (nA)	7.76 ± 0.72 ¶	6.74 ± 0.33	6.44 ± 0.61	*2.89 ± 0.67*
relA1 (%)	40 ± 3	31 ± 1 *	20 ± 2 **	-
relA2 (%)	35 ± 3	37 ± 1	45 ± 2 **	*24 ± 9*
relA3 (%)	25 ± 2	32 ± 1 *	35 ± 3 *	*76 ± 9*
Cap (pF)	142 ± 12 ¶	155 ± 5	172 ± 12	*196 ± 23*
D1 (pA/pF)	21.5 ± 2.2	13.1 ± 0.8 *	7.8 ± 1.1 **	-
D2 (pA/pF)	18.9 ± 2.4	16.9 ± 1.2	17.4 ± 2.1	*4.3 ± 2.9*
D3 (pA/pF)	12.9 ± 0.8	13.1 ± 0.5	11.9 ± 1.0	*10.5 ± 2.0*
D0 (pA/pF)	2.0 ± 0.5	1.5 ± 0.2	2.2 ± 0.3	*1.0 ± 0.6*
DΣ (pA/pF)	55.3 ± 3.1	44.7 ± 2.0 *	39.1 ± 3.9 *	*15.7 ± 5.3*
	(n = 16)	(n = 67)	(n = 14)	*(n = 3)*
Recovery from inactivation				
$\tau_{rec}1$(ms)	73.2 ± 3.3 ¶	71.0 ± 2.6	339 ± 29 **	*855*
$\tau_{rec}2$ (ms)	1365 ± 87	1156 ± 31	1792 ± 139 **	*2742*
$A_{rec}1$ (%)	65 ± 2	53 ± 1 *	49 ± 4 *	*58*
$A_{rec}2$ (%)	35 ± 2	47 ± 1 *	51 ± 4 *	*42*
	(n = 13)	(n = 61)	(n = 9)	*(n = 1)*
Voltage dependence of inactivation				
$V_{1/2}1$ (mV)	-59.3 ± 2.1 ¶	-56.5 ± 1.4	-75.7 ± 4.3 **	*-90.9*
$V_{1/2}2$ (mV)	-37.6 ± 1.9	-35.6 ± 0.6	-38.7 ± 1.2	*-40.8*
A_V1 (%)	58 ± 6	52 ± 3	12 ± 2 **	*13*
A_V2 (%)	42 ± 6	48 ± 3	88 ± 2 **	*87*
	(n = 11)	(n = 55)	(n = 9)	*(n = 1)*

Analysis results obtained for current kinetics and magnitudes, recovery from inactivation and voltage dependence of inactivation for female myocytes with different KChIP2 genotypes.

¶ significantly different from male myocytes (unpaired Student's *t*-test);

* significantly different from KChIP2$^{+/+}$;

** significantly different from both KChIP2$^{+/+}$ and KChIP2$^{+/-}$ (one way ANOVA);

§ significantly different from RMS_{2exp} (paired Student's *t*-test); abbreviations are explained in the text.

doi:10.1371/journal.pone.0171213.t002

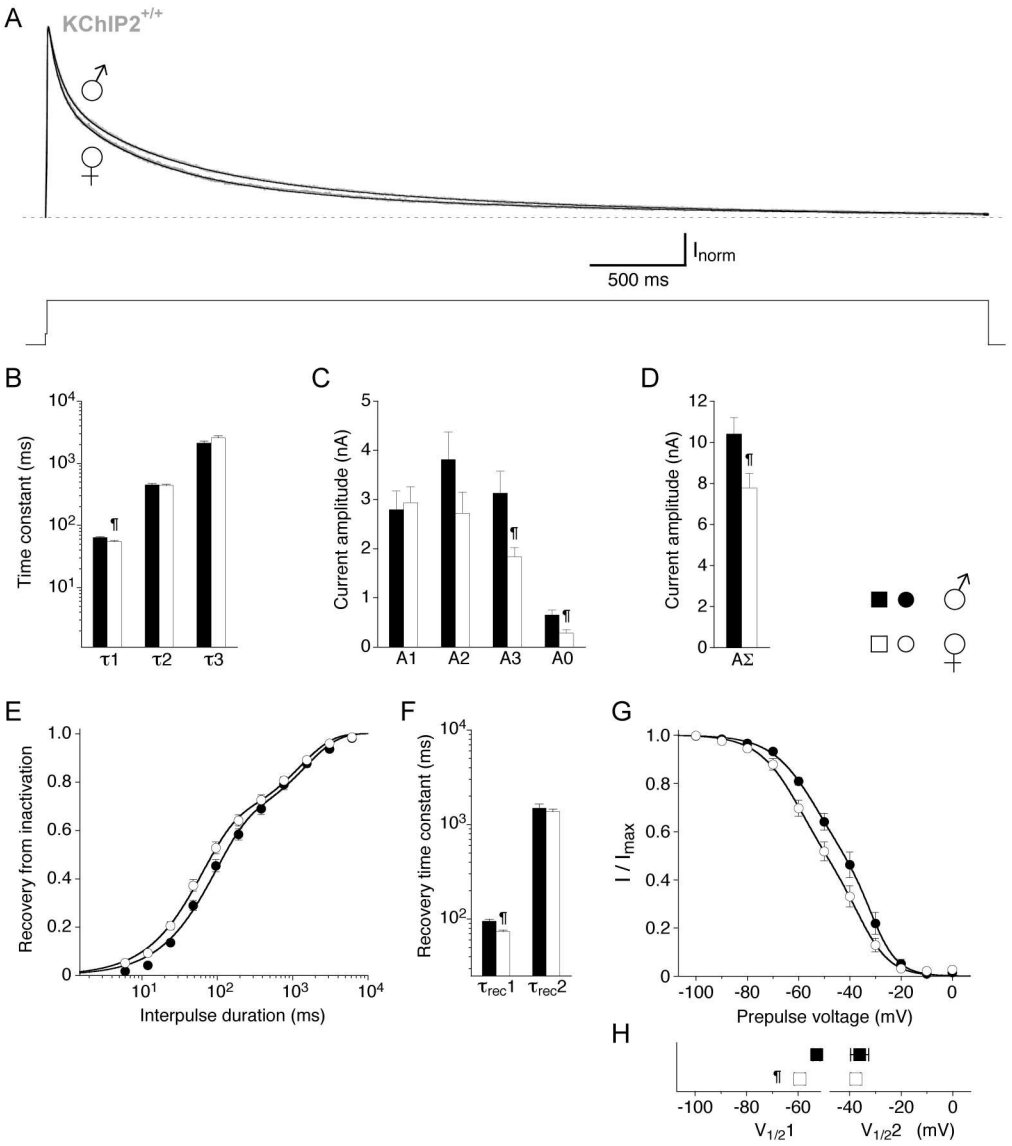

Fig 5. Comparison of outward current inactivation properties in male and female wild-type myocytes. For the compound outward current in male and female wild-type ($KChIP2^{+/+}$) myocytes the kinetics of macroscopic inactivation, the kinetics of recovery from inactivation and the voltage dependence of inactivation were compared. Data from male myocytes are depicted as black symbols, data from female myocytes as empty symbols. **A.** Representative outward current traces from a male and a female $KChIP2^{+/+}$ myocyte, respectively, recorded during a 5 s voltage pulse to +40 mV (voltage protocol shown below current traces; dotted line represents non-inactivating current level). For both sexes $KChIP2^{+/+}$ outward current decay kinetics were best described by a triple-exponential function. Note the slightly faster decay kinetics in the female myocyte. **B.** Mean time constants obtained with a triple-exponential function (τ1, τ2 and τ3). **C.** Mean amplitudes of the individual time constants obtained by triple-exponential fitting (A1, A2 and A3) and the amplitude of the non-inactivating current component (A0). **D.** Mean total amplitude of the compound outward current (AΣ). **E.** Recovery data fitted by a double-exponential function. Note that for female $KChIP2^{+/+}$ myocytes the recovery from inactivation was apparently faster. **F.** Mean recovery time constants ($\tau_{rec}1$ and $\tau_{rec}2$) obtained by double-exponential fitting. **G.** Data describing the voltage dependence of inactivation fitted with the sum of two Boltzmann-functions. Note the apparent negative shift of the fitting curve in female relative to male $KChIP2^{+/+}$ myocytes. **H.** Mean values for $V_{1/2}1$ and $V_{1/2}2$ obtained with the sum of two Boltzmann-functions (¶, unpaired Student's *t*-test).

doi:10.1371/journal.pone.0171213.g005

smaller than the one found in male myocytes. The intermediate and slow decay kinetics showed no gender-dependent differences (Fig 5B and Table 2). In female myocytes the I_{to} amplitude A1 was 2.93 ± 0.33 nA (n = 16), comparable to male myocytes (Fig 5C), however, the amplitudes A3 and A0, and, accordingly, the total amplitude of the compound outward current AΣ were smaller than in male myocytes (Fig 5C and 5D and Table 2). Due to the smaller cell size of female myocytes, these differences are not reflected in the current densities (Table 2). The kinetics of recovery from inactivation appeared faster in female myocytes (Fig 5E). This was due to a smaller $\tau_{rec}1$ value (73.2 ± 3.3 ms, n = 13). The second recovery component ($\tau_{rec}2$ = 1365 ± 87 ms, n = 13) was not different from male myocytes (Fig 5F and Table 2). The voltage dependence of inactivation appeared negatively shifted in female myocytes (Fig 5G), which was due to a more negative $V_{1/2}1$ value (-59.3 ± 2.1 mV, n = 11). The second (less negative) component of the voltage dependence ($V_{1/2}2$ = -37.6 ± 1.9 mV, n = 11) was not different from male myocytes (Fig 5H and Table 2).

Fig 6A shows the inactivating components of normalized current traces recorded at +40 mV from female myocytes with different KChIP2 genotypes. In general, the decay kinetics and KChIP2 genotype-specific features of outward currents in female myocytes were similar to the ones found for male myocytes: Currents from female KChIP2$^{+/+}$ myocytes exhibited the fastest decay kinetics, while KChIP2$^{+/-}$ and KChIP2$^{-/-}$ showed slower decay kinetics. Outward current decay was best described by a triple-exponential function for all KChIP2 genotypes, but in a fraction of female KChIP2$^{-/-}$ myocytes (3 out of 17) current decay was extremely slow and could be sufficiently well described by a double-exponential function (Fig 6A). The fit results for female myocytes are shown in Fig 6B and 6C. In female KChIP2$^{+/-}$ myocytes the I_{to} kinetics (τ1 = 58.2 ± 1.3 ms, n = 67) were not significantly different from KChIP2$^{+/+}$, whereas KChIP2$^{-/-}$ I_{to} kinetics (τ1 = 70.3 ± 7.0 ms, n = 14) were slower (Fig 6B and Table 2). In female myocytes I_{to} amplitude also showed a clear KChIP2 gene dosage effect with A1 = 1.94 ± 0.11 nA (n = 67) for KChIP2$^{+/-}$ and A1 = 1.23 ± 0.15 nA (n = 14) for KChIP2$^{-/-}$ (Fig 6C and Table 2), which was also reflected in the current densities (Table 2). Also similar to male myocytes, neither the intermediate nor the slow decay kinetics showed a dependence on the KChIP2 genotype, however, in female myocytes this applied also to their amplitudes, including A0, and densities (Fig 6B and 6C and Table 2). Therefore, the total amplitude of the compound outward current AΣ was not significantly different among the three KChIP2 genotypes (Fig 6D and Table 2), albeit the corresponding densities proved to be significantly reduced in female KChIP2$^{+/-}$ and KChIP2$^{-/-}$ myocytes (Table 2). In the female KChIP2$^{-/-}$ myocytes with an apparent loss of I_{to} the time constants of the fast and slow decay component obtained with double-exponential fitting also closely resembled the time constants of the intermediate and slow decay component obtained for all other myocytes with triple-exponential fitting (Fig 6B). However, the amplitude of the fast component obtained with double-exponential fitting was apparently reduced, and, accordingly, the total amplitude $A\Sigma$ appeared smaller in these female KChIP2$^{-/-}$ myocytes (Fig 6C and 6D; no statistical tests performed).

Like in male myocytes the kinetics of recovery of the compound outward current from inactivation in female myocytes were best described by the sum of two exponential functions for all three KChIP2 genotypes (Fig 7A). The recovery kinetics differed for female KChIP2$^{+/-}$ and KChIP2$^{+/+}$ myocytes. While the time constants in KChIP2$^{+/-}$ ($\tau_{rec}1$ = 71.0 ± 2.6 ms, $\tau_{rec}2$ = 1156 ± 31 ms) were similar to KChIP2$^{+/+}$ (Fig 7B), their relative contributions were shifted in favor of the slow recovery component ($A_{rec}1$ = 53%, $A_{rec}2$ = 47%, n = 61; Fig 7C). Female KChIP2$^{-/-}$ and KChIP2$^{+/-}$ myocytes shared this new distribution of relative amplitudes, however, in the KChIP2$^{-/-}$ myocytes the recovery time constants were larger ($\tau_{rec}1$ = 339 ± 29 ms, 49%; $\tau_{rec}2$ = 1792 ± 139 ms, 51%, n = 9) resulting in a further slowing of the recovery kinetics (Fig 7A–7C and Table 2). Also similar to male myocytes, the voltage dependence of

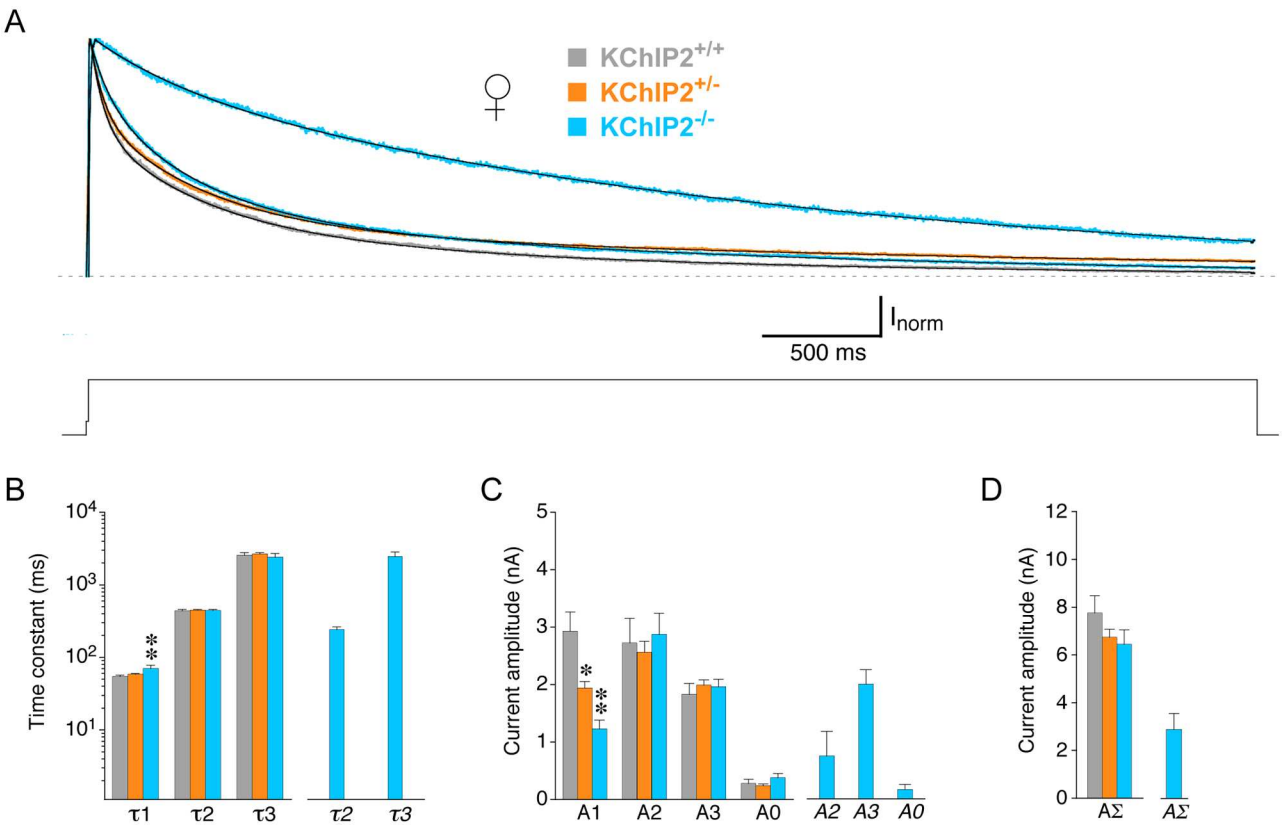

Fig 6. Analysis of macroscopic inactivation in female myocytes with different KChIP2 genotypes. Outward currents were activated by 5 s voltage pulses from -80 to +40 mV in female KChIP2$^{+/+}$, KChIP2$^{+/-}$ and KChIP2$^{-/-}$ myocytes. **A.** Representative current traces for the different KChIP2 genotypes were normalized to peak and only the inactivating current components are shown (voltage protocol below current traces; dotted line represents non-inactivating current level). Current decay kinetics in KChIP2$^{+/+}$ (grey), KChIP2$^{+/-}$ (orange) and most KChIP2$^{-/-}$ myocytes (14 out of 17, blue, fast decay) were best described by a triple-exponential function. In some KChIP2$^{-/-}$ myocytes (3 out of 17, blue, slow decay) a double-exponential function was sufficient. **B.** Mean time constants obtained with a triple-exponential function (τ1, τ2 and τ3) for female KChIP2$^{+/+}$ (grey bars), KChIP2$^{+/-}$ (orange bars) and most KChIP2$^{-/-}$ myocytes (14 out of 17, blue bars), and mean time constants obtained with a double-exponential function for 3 out of 17 female KChIP2$^{-/-}$ myocytes (*τ2* and *τ3*, separate blue bars on the right). **C.** Mean amplitudes of the individual time constants obtained by triple-exponential (A1, A2 and A3) and double-exponential fitting (*A2* and *A3*, separate bars on the right) and mean amplitudes of the corresponding non-inactivating current components (A0, *A0*). Like in male myocytes, there was a gene dosage effect on A1 in female myocytes (* significantly different from KChIP2$^{+/+}$; ** significantly different from both KChIP2$^{+/+}$ and KChIP2$^{+/-}$; one-way ANOVA). **D.** Mean total amplitudes of the compound outward current (AΣ, *AΣ*). The KChIP2 gene dosage effect observed for A1 is not reflected in AΣ in female myocytes.

doi:10.1371/journal.pone.0171213.g006

compound outward current inactivation was best described by the sum of two Boltzmann-functions for all KChIP2 genotypes in female myocytes (Fig 7D). No significant differences relative to KChIP2$^{+/+}$ were detected for the KChIP2$^{+/-}$ fit values ($V_{1/2}1$ = -56.5 ± 1.4 mV, 52%; $V_{1/2}2$ = -35.6 ± 0.6 mV, 48%; n = 55; Fig 7E and Table 2), although the corresponding inactivation curves apparently differ (Fig 7D). In KChIP2$^{-/-}$ myocytes $V_{1/2}1$ was shifted negative (-75.7 ± 4.3 mV) and the relative contribution was reduced to 12% in favor of the second (less negative) component ($V_{1/2}2$ = -38.7 ± 1.2, 88%; n = 9; Fig 7E and 7F). Taken together, there were no qualitative differences between the data obtained for male and female KChIP2$^{+/+}$ myocytes. However, I_{to} decay kinetics and the recovery from inactivation were faster and the first (more negative) component of the voltage dependence was more negative in female than in male KChIP2$^{+/+}$ myocytes. Concerning the KChIP2 genotype dependence, the same effects, including a clear KChIP2 gene dosage effect on I_{to} magnitude but not on inactivation

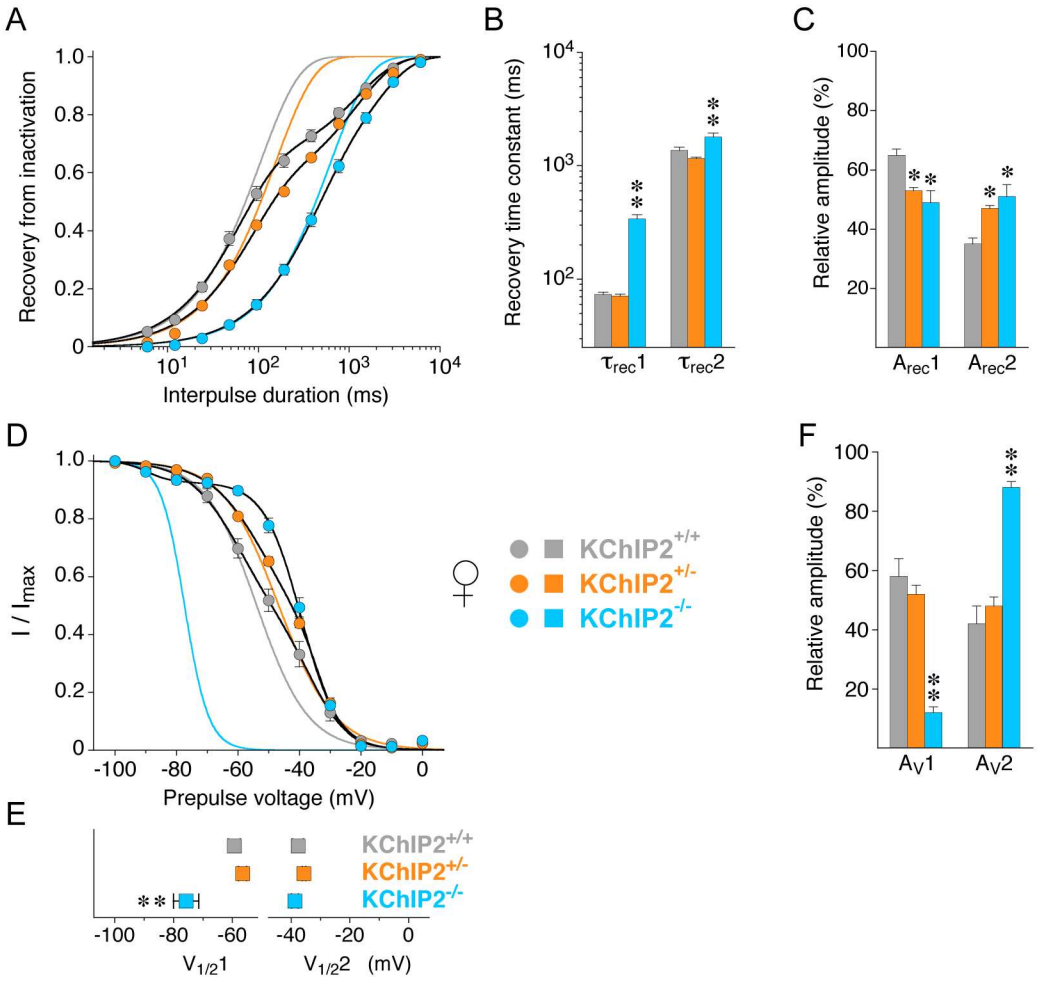

Fig 7. Recovery from inactivation and voltage dependence of inactivation in female myocytes with different KChIP2 genotypes. Recovery from inactivation and the voltage dependence of inactivation were studied in female KChIP2$^{+/+}$ (grey symbols), KChIP2$^{+/-}$ (orange symbols) and KChIP2$^{-/-}$ myocytes (blue symbols). **A.** Recovery plots. Fitting curves represent double-exponential functions. Lines without symbols represent single-exponential functions fitted to a fraction of the data points (the fast component) and forced to reach 1. Note that in female myocytes a moderate apparent slowing of the recovery kinetics was observed for KChIP2$^{+/-}$ compared to KChIP2$^{+/+}$. **B.** Mean recovery time constants ($\tau_{rec}1$ and $\tau_{rec}2$) obtained by fitting the recovery kinetics with a double-exponential function. **C.** Mean relative amplitudes of recovery time constants for all KChIP2 genotypes ($A_{rec}1$ and $A_{rec}2$). **D.** Inactivation curves. The data were fitted with the sum of two Boltzmann-functions. Lines without symbols represent single Boltzmann-functions fitted to a fraction to the data points (the more negative portion) and forced to reach 0. **E.** Mean values for $V_{1/2}1$ and $V_{1/2}2$ obtained with the sum of two Boltzmann-functions. Note that $V_{1/2}2$ values are similar in all KChIP2 genotypes. **F.** Mean relative amplitudes of the voltage dependences defined by $V_{1/2}1$ and $V_{1/2}2$ (A_v1 and A_v2); * significantly different from KChIP2$^{+/+}$; ** significantly different from both KChIP2$^{+/+}$ and KChIP2$^{+/-}$; one-way ANOVA.

doi:10.1371/journal.pone.0171213.g007

properties, were seen in male and female myocytes, albeit inactivation properties slightly differed for female KChIP2$^{+/+}$ and KChIP2$^{+/-}$ myocytes.

Heterologous coexpression of Kv4.2 and KChIP2

We asked whether the partial KChIP2 gene dosage effect on I_{to} seen in cardiomyocytes (i.e., heterozygous deletion of the KChIP2 gene has a strong effect on current magnitude but no or only a moderate effect on inactivation) can be reproduced with recombinant channel proteins

in a heterologous expression system. For this purpose we expressed Kv4.2 in the absence or presence of KChIP2 in *Xenopus* oocytes, by injecting predefined cRNA amounts, and measured currents with the two-electrode voltage-clamp technique (see Materials and Methods). We were particularly interested in the dynamics of KChIP2 effects on Kv4.2-mediated current amplitudes and Kv4.2 inactivation kinetics. In order to establish appropriate experimental conditions, we first injected, into individual oocytes, 1 ng Kv4.2 cRNA either alone or in combination with 1 ng KChIP2 cRNA, measured the peak current amplitudes 24, 48, 72 and 96 h after cRNA injection and generated corresponding expression profiles (see S2A Fig). The results showed that using 1 ng per oocyte of Kv4.2 cRNA and measuring currents between 24 and 96 h after cRNA injection yields currents with decent amplitudes (between 1 and 40 μA) amenable to modulation by KChIP2 coexpression (5- to 7-fold gain in amplitude, see S2B Fig; [8, 14]). Next, we coinjected different amounts of KChIP2 cRNA (0–12.8 ng) with a fixed amount of 1 ng Kv4.2 cRNA into individual oocytes and measured currents 48 h after cRNA injection (Fig 8A). The peak amplitude of the currents showed a clear dependence on the amount of KChIP2 cRNA coinjected per oocyte (Fig 8F). The dependence was steep with lower amounts (e.g., 0.2 ng: 8.1 ± 0.6 μA, n = 9; 0.4 ng: 12.8 ± 1.6 μA, n = 7) and more shallow with higher amounts of KChIP2 cRNA (e.g., 3.2 ng: 24.9 ± 1.7 μA; 6.4 ng: 27.9 ± 2.5 μA, n = 9; see also S3A Fig). We also analysed macroscopic inactivation kinetics and the kinetics of recovery from inactivation (Fig 8B and 8C). For both parameters the KChIP2 dependence was obvious, with a slowing of macroscopic inactivation and an acceleration of recovery from inactivation in the presence of KChIP2, in accordance with published results [8, 14]. However, in contrast to the peak current amplitude (Fig 8F), macroscopic inactivation and recovery from inactivation showed only a vestigial dose dependence in the low to intermediate range of KChIP2 cRNA amounts and no dose dependence at all (i.e., the effects on inactivation gating were saturated) when cRNA amounts larger than 1.6 ng were coinjected with 1 ng Kv4.2 cRNA per oocyte (Fig 8B, 8C, 8G and 8H and S3 Fig). These findings are reminiscent of the KChIP2 gene dosage effect seen in cardiomyocytes for I_{to} magnitude but not for inactivation properties (see Discussion).

To further explore the dynamics of the Kv4.2/KChIP2 interaction we injected Kv4.2 and KChIP2 cRNAs (both 1 ng) at different time points into the same oocyte. After the initial injection of Kv4.2 cRNA, channels were allowed to assemble and get intalled in the plasma membrane in the absence of KChIP2 for 48 h. After this time KChIP2 cRNA was injected and currents were recorded either another 5 h (48+5) or another 48 h later (48+48). After 48 h of KChIP2 expression there was a clear gain in amplitude (compare Fig 8F and S2A Fig), macroscopic inactivation was slowed (Fig 8G), and recovery from inactivation was accelerated (Fig 8H). As expected, due to the KChIP2 cRNA amount of only 1 ng per oocyte, none of the KChIP2 effects on inactivation gating reached saturation. After 5 h of KChIP2 expression no gain in amplitude was apparent (Fig 8F), however, macroscopic inactivation was moderately slowed (Fig 8D and 8G) and recovery from inactivation moderately accelerated (Fig 8E and 8H). Notably, after 5 h the recovery kinetics exhibited a small (~ 15%) slow component, which was not captured by the single-exponential fit (Fig 8E), possibly representing a small amount of KChIP2-less Kv4.2 channels residing in the oocyte membrane. These results raise the question whether preexisting Kv4.2 channels in the oocyte membrane can be subsequently modified by KChIP2 (see Discussion).

Discussion

We have shown in murine left ventricular myocytes a distinct KChIP2 gene dosage effect on I_{to} magnitude (i.e., amplitude and density). Inactivation properties (i.e., inactivation kinetics,

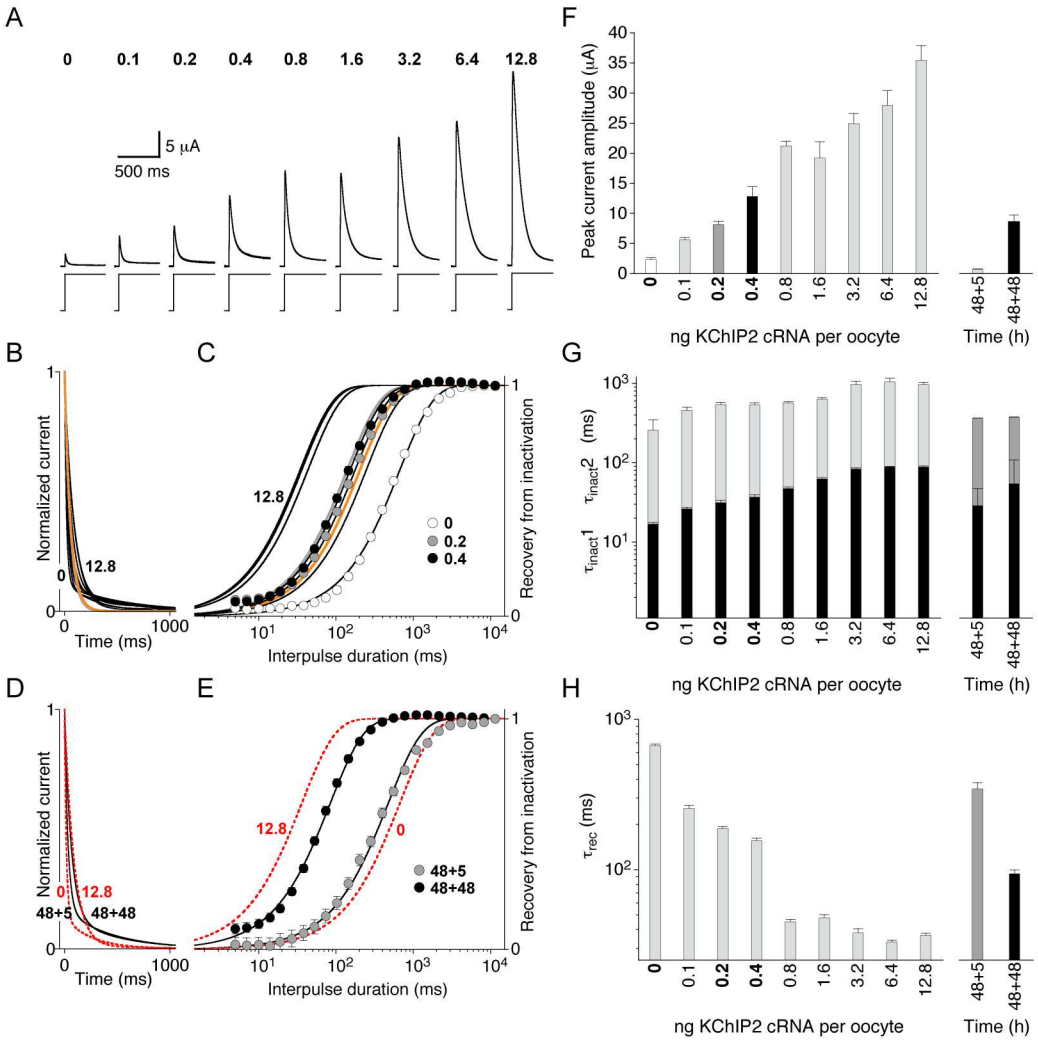

Fig 8. Expression of Kv4.2 and KChIP2 in *Xenopus* oocytes. Two-electrode voltage-clamp experiments were performed on individual oocytes following cRNA injection. **A.** Currents obtained with depolarizing voltage jumps from -80 to +40 mV (voltage protocols below traces) 48 h after cRNA injection. Different amounts of KChIP2 cRNA (ng per oocyte indicated above traces) were coinjected with a fixed amount of Kv4.2 cRNA (1 ng per oocyte). Note the tight correlation between KChIP2 cRNA amount and peak current amplitude. **B.** Idealized current traces based on the mean fit results obtained with a double-exponential function (Kv4.2/KChIP2-mediated currents with 0–12.8 ng KChIP2 cRNA coinjected: black) and based on the mean τ1 values from triple-exponential fits (i.e., the I_{to} component) of female myocytes ($KChIP2^{+/+}$: grey, $KChIP2^{+/-}$: orange). All currents were normalized to peak. **C.** Recovery from inactivation at -80 mV obtained for oocytes injected with different amounts of KChIP2 cRNA. Pooled recovery data are shown for oocytes injected with 1 ng Kv4.2 cRNA and 0 ng (empty symbols), 0.2 ng (grey symbols) and 0.4 ng KChIP2 cRNA (black symbols). Kv4.2/KChIP2 recovery kinetics were fitted by a single-exponential function. Black lines without symbols: Single-exponential fits for all other KChIP2 cRNA amounts (0.1, 0.8, 1.6, 3.2, 6.4 and 12.8 ng per oocyte); colored lines without symbols: Single-exponential functions representing the fast recovery component of female myocytes (see Fig 7A; $KChIP2^{+/+}$: grey, $KChIP2^{+/-}$: orange). **D.** Idealized current traces based on the same fitting procedures as the currents in B; black traces: currents obtained after consecutive injection of 1 ng Kv4.2 and 1 ng KChIP2 cRNA into the same oocyte; faster decay: 48 h Kv4.2 expression followed by 5 h KChIP2 expression (48+5); slower decay: 48 h Kv4.2 expression followed by 48 h KChIP2 expression (48+48). Red dotted traces represent the data for 0 and 12.8 ng KChIP2 cRNA from B. **E.** Recovery from inactivation for the two experimental paradigms (grey symbols: 48+5; black symbols: 48+48). The data were fitted by a single-exponential function. Red dotted lines: single exponential fits to the recovery data obtained with 0 and 12.8 ng KChIP2 cRNA per oocyte). Note the slow recovery component (~ 15%) in the 48+5 data, which was not captured by the single-exponential fit. **F.** Mean peak current amplitudes from A and from the experiments with consecutive cRNA injection (48+5 and 48+48). **G.** Inactivation time constants ($\tau_{inact}1$ and $\tau_{inact}2$) from B (0–12.8 ng KChIP2 cRNA per oocyte) and D (48+5 and 48 +48). **H.** Recovery time constants (τ_{rec}) from C (0–12.8 ng KChIP2 cRNA per oocyte) and E (48+5 and 48+48).

doi:10.1371/journal.pone.0171213.g008

kinetics of recovery from inactivation and voltage dependence of inactivation), on the other hand, were found to be similar in KChIP2$^{+/+}$ and KChIP2$^{+/-}$ myocytes. Only in KChIP2$^{-/-}$ myocytes inactivation and recovery from inactivation were slowed and a portion of the voltage dependence of inactivation was shifted to more negative potentials. No qualitative differences concerning the KChIP2 genotype-dependent remodeling have been observed between male and female myocytes.

Isolation of I_{to} properties: Technical aspects

In order to isolate I_{to} from the compound outward current in murine cardiomyocytes and to measure its amplitude and decay kinetics a prepulse-inactivation-subtraction method has been frequently used ([9, 23, 27, 28]; see also Fig 1A and S1 Fig of the present study). This method relies on the complete inactivation of I_{to}-related potassium channels by a depolarizing prepulse which must not gate any other potassium channels. Therefore, both prepulse length and prepulse voltage are critical parameters. Typically, prepulse lengths between 75 ms [9] and 120 ms [27] and a prepulse voltage of -40 mV have been used. In the present study the prepulse-inactivation-subtraction method was applied to male myocytes using a prepulse length of 160 ms and a prepulse voltage of -40 mV (Fig 1A and S1 Fig). We obtained smaller I_{to} densities for wild-type myocytes (S1 Table) than reported in the literature based on the same method with test potentials between +30 and +50 mV (25–35 pA/pF; [9, 23, 27, 28]). Our isolated I_{to} kinetics (S1 Table) were comparable to the ones found by Tozakidou et al. (τ = 52 ms; [27]) but slower than the ones found by Brouillette et al. (τ = 28 ms; [23]). The prepulse-inactivation-subtraction method has several disadvantages: The requirements concerning prepulse length and prepulse voltage may depend on experimental conditions, such as the tissue from which the myocytes were isolated (e.g., apex vs. septum or endocard vs. epicard), age and gender of the mice, but also their genotype and genetic background (i.e., wild-type vs. mutant, different mouse strains). Therefore, the method cannot be reliably used without validating the settings for each experimental condition by measuring the amount and kinetics of inactivation at the prepulse potential [23]. But even if these experimental requirements are met, the prepulse-inactivation-subtraction method yields limited information on other inactivating and non-inactivating current components, which may be remodeled as part of the experiment. Therefore, this isolation method is not very well suited to compare the different genotypes of an I_{to}-related transgenic mouse model.

As an alternative method many investigators apply long depolarizing pulses to activate all components of the outward current and let them inactivate one by one over many seconds [24–26]. Then, based on multi-exponential fitting of the current decay, multiple time constants and their amplitudes are obtained, and the individual decay components can be assigned to individual current components [24–26]. Of course, this method depends critically on the length of the depolarizing pulse and on the number of exponential terms deployed. Based on double-exponential fitting of the compound outward currents obtained with 4.5 s pulses, the terms $I_{to,f}$ (fast transient outward current, first decay component in the majority of cells), $I_{to,s}$ (slow transient outward current, first decay component in a subset of cells), $I_{K,slow}$ (slowly inactivating current, second decay component) were coined by Guo et al. [24] and Xu et al. [26], in addition to the non-inactivating steady-state current component I_{SS}. Triple-exponential fitting was utilized by these authors only to describe the current decay kinetics in cells from left ventricular septum (but not apex) to account for the putative presence of both $I_{to,f}$ and $I_{to,s}$ [24, 26]. By contrast, Liu and coworkers used rigorous triple-exponential fitting to describe the decay kinetics of currents obtained with pulse lengths between 5 and 25 s from all ventricular myocytes [25]. These authors state that $I_{to,f}$ and $I_{to,s}$ cannot be kinetically separated

based on macroscopic inactivation, and thus, the first of three decay components represents either $I_{to,f}$ or $I_{to,s}$ or a mixture of the two [25]. For the second and third decay component the terms $I_{K,slow1}$ and $I_{K,slow2}$, respectively, were coined [25]. As an unbiased way to find out which of the two fitting methods is better suited to describe our data, we initially applied them in parallel to male KChIP2$^{+/+}$ myocytes and compared the results with the ones obtained by the prepulse-inactivation-subtraction method (see Fig 1). Due to significantly lower RMS values and the perfect match between τs and τ1 and between As and A1 we decided to use triple-exponential fitting for all myocytes of the present study if appropriate. Therefore, we like to adhere to the classification and nomenclature of inactivating current components used by Liu and coworkers (τ1 and A1: I_{to}; τ2 and A2: $I_{K,slow1}$; τ3 and A3: $I_{K,slow2}$; [25]). In our study double-exponential fitting was only appropriate for the currents obtained from a small fraction of KChIP2$^{-/-}$ myocytes, suggesting the loss of one current component (see below).

Due to peak amplitudes of ~ 10 nA (Tables 1 and 2) it cannot be excluded that the currents obtained with our whole-cell patch-clamp recordings are to some degree distorted by insufficient series resistance compensation (see Materials and Methods). Also, I_{K1}-mediated tail currents were often seen upon repolarization, indicative of K^+ accumulation in t-tubules and consequently a shift in E_K ([29]; see for instance Fig 3). Despite these potential sources of error, our triple-exponential fit results for wild-type myocytes are in very good agreement with the ones obtained based on the same analysis method by Liu et al. using 5 s pulses (mean I_{to} time constant ~ 55 ms; [25]) and by Costantini et al. using 3.5 s pulses (mean I_{to} density ~ 18 pA/pF; [30]). Liu and coworkers found out that maximal reliability of the triple-exponential fit is reached with pulse lengths greater than 20 s [25]. With 25 s pulses to +60 mV their mean I_{to} inactivation time constant was 54 ms and their mean I_{to} density 24 pA/pF, still very close to our results (see Tables 1 and 2). Our $I_{K,slow1}$ and $I_{K,slow2}$ time constants may be understimated due to the shorter pulse length of 5 s used in the present study, whereas the on average smaller current densities may be explained by our test potential of +40 mV instead of +60 mV [25, 30].

In the present study multi-exponential fitting was not applied to the test pulse currents obtained with the double-pulse protocol and the variable prepulse protocol to study recovery from inactivation and the voltage dependence of inactivation, respectively. Rather, these inactivation properties were cumulatively determined for the compound outward current by processing the relative peak amplitudes of the test pulse currents. To account for the presence of current components with different recovery kinetics and different voltage dependences of inactivation the data were fitted with a double-exponential function (recovery from inactivation) and the sum of two Boltzmann-functions (voltage dependence of inactivation). At the expense of this simplification we were able to acquire data from a large number of cells with minimal SEM, a favorable condition to perform ANOVA over multiple groups. Aware that either recovery component and either component of the voltage dependence of inactivation may reflect more than one current component, we assumed that I_{to} properties were merely represented by the faster recovery component ($\tau_{rec}1$), at least for KChIP2$^{+/+}$. Our values for $\tau_{rec}1$ (see Tables 1 and 2) are larger than most values obtained for the isolated I_{to} component (recovery time constants between 25 and 50 ms; [23–26, 31–33]). We cannot exclude that our $\tau_{rec}1$ values are influenced by the fast $I_{K,slow1}$ recovery component and/or $I_{K,slow2}$ recovery kinetics ([25]; see below). On the other hand, $\tau_{rec}1$ values cumulatively obtained by Tozakidou et al. (51 ms; [27]) and by Wang & Duff (41 ms; [34]) for the compound outward current, as in the present study, are virtually identical to the $I_{to,f}$ recovery time constant determined by Foeger et al. (51 ms; [31]), which warrants our simplified approach. A further assumption of the present study was that I_{to} properties are represented by the more negative component of the voltage dependence of inactivation ($V_{1/2}1$). After all, $V_{1/2}1$, rather than $V_{1/2}2$, was modified in

a KChIP2 genotype-dependent manner (see below). But appart from that, the assumption is directly related to the -40 mV prepulse used to completely inactivate I_{to}, meaning that the corresponding $V_{1/2}$ value must be more negative than that. In fact, our $V_{1/2}1$ values (see Tables 1 and 2) are very similar to the one obtained by Brouiette et al. (-56 mV, [23]) for the I_{to} component isolated with the prepulse-inactivation-subtraction method.

Remodeling in I_{to}-related transgenics

There are now good protein candidates for the molecular correlates of individual inactivating current components in murine left ventricular myocytes [1, 35]: $I_{to,f}$ is thought to be mainly carried by Kv4.2 channels associated with KChIP2 (fast recovery from inactivation), and $I_{to,s}$ by Kv1.4 channels (slow recovery from inactivation). Both Kv4.2/KChIP2 and Kv1.4 channels may potentially contribute to I_{to}, although in most wild-type cardiomyocytes Kv4.2/KChIP2-mediated $I_{to,f}$ governs I_{to} (see below). $I_{K,slow1}$ is thought to be carried by Kv1.5 channels and $I_{K,slow2}$ by Kv2.1 channels. In order to unveil the molecular correlate of the I_{to} component(s) in murine cardiomyocytes, different transgenic mouse models were deployed. Initially, it was found that targeted deletion of the Kv1.4 gene ($Kv1.4^{-/-}$) left I_{to} virtually unaffected [36], showing that I_{to} consists mainly of $I_{to,f}$ for which Kv1.4 is an unlikely candidate. By contrast, I_{to} was strongly reduced by tissue-specific overexpression of a dominant-negative Kv4.2 pore mutant (Kv4.2W362F; [3, 24]) or N-terminal fragment (Kv4.2S1-S4; [37]), showing that the $I_{to,f}$ component is carried by members of the Kv4 subfamily. Finally, targeted deletion of the Kv4.2 gene ($Kv4.2^{-/-}$; [38]) and the Kv4.3 gene ($Kv4.3^{-/-}$; [33]), respectively, demonstrated that $I_{to,f}$ is carried mainly by Kv4.2 rather than Kv4.3 in mice. Notably, it has been recognized early on that dominant-negative Kv4.2W362F expression causes remodeling processes in the form of $I_{to,s}$ up-regulation [3, 39], which was not seen in cardiomyocytes from mice overexpressing Kv4.2W362F in a $Kv1.4^{-/-}$ genetic background ($Kv4.2W362FXKv1.4^{-/-}$; [39]). These results led to the conclusion that Kv1.4 channels are responsible for $I_{to,s}$ up-regulation. An emergence of $I_{to,s}$ was also observed in $Kv4.2^{-/-}$ myocytes, however, specific deletion of the Kv4.2 gene may allow the up-regulation of a Kv4.3-mediated $I_{to,f}$ [32].

Targeted deletion of the KChIP2 gene ($KChIP2^{-/-}$; [9, 21, 31, 40]) has been used to study the role of KChIP2 in I_{to} expression, the present study included. Initially, Kuo and coworkers reported a complete loss of I_{to} for the homozygous KChIP2 knockout ($KChIP2^{-/-}$), although, based on the results of the prepulse-inactivation-subtraction method, a not further quantified "background level" of I_{to} was apparently left in the $KChIP2^{-/-}$ myocytes [9]. This is very similar to our results, when using the prepulse-inactivation-subtraction method (see S1 Fig and S1 Table). However, a clear separation of two different $KChIP2^{-/-}$ myocyte populations, one with a complete loss of I_{to} and one with a kinetically modified I_{to}, may only be possible by multi-exponential fitting. Analogous to our multi-exponential fitting strategy, Foeger et al. deployed the same number of exponential terms to describe the compound outward current decay kinetics in $KChIP2^{+/+}$ and $KChIP2^{-/-}$ myocytes [31]. Both the results of prepulse-inactivation-subtraction and the results of multi-exponential fitting can be interpreted as an up-regulation of a novel (or previously hidden) current component in $KChIP2^{-/-}$ myocytes in the absence of Kv4.2 channel-mediated $I_{to,f}$. The results are comparable to the ones obtained with dominant-negative Kv4.2W362F expression [3, 24] or with the $Kv4.2^{-/-}$ deletion mutant [38] and may be explained by $I_{to,s}$ up-regulation [31]. Notably, for a minor fraction of $KChIP2^{-/-}$ myocytes we reduced the number of exponential terms (double-exponential instead of triple-exponential) in order to obtain decent fit results. It is intriguing that double-exponential analysis of the currents obtained from these $KChIP2^{-/-}$ myocytes apparently yielded the $I_{K,slow1}$ and $I_{K,slow2}$ components. We think that only these myocytes underwent a complete loss of I_{to}, meaning that

$I_{to,f}$ was eliminated and $I_{to,s}$ not up-regulated, reminiscent of the current kinetics found in Kv4.2W362FXKv1.4$^{-/-}$ myocytes [39].

Deviding the (novel) $I_{to,s}$ density by the (native) $I_{to,f}$ density represents a possibility to quantify I_{to} remodeling for a given experimental approach. Notably, this rough estimate yields relatively uniform results when applied to various published data: Foeger et al. found a fraction of 0.421 for myocytes of KChIP2$^{-/-}$ left ventricular apex [31], meaning that after the complete loss of $I_{to,f}$, up-regulation of the novel current component restores 42.1% of the native $I_{to,f}$ density. Barry et al. found a fraction of 41.3% for myocytes expressing Kv4.2W362F [3] and Guo et al. a fraction of 38.4% in Kv4.2$^{-/-}$ myocytes [38]. Intriguingly, even in naive myocytes devoid of $I_{to,f}$ the relative $I_{to,s}$ fraction, compared to $I_{to,f}$-expressing cells, is 43.5% [26]. In the present study, deviding D1 of KChIP2$^{-/-}$ myocytes by D1 of KChIP2$^{+/+}$ myocytes (see Tables 1 and 2) as an estimate of the $I_{to,s}/I_{to,f}$ fraction yielded 31.4% for male and 36.3% for female myocytes. These values are a little lower than the one obtained by Foeger et al. for KChIP2$^{-/-}$ myocytes [31] but correlate extremely well with the fraction of 31.6% obtained by Liu et al. for Kv4.2$^{-/-}$ myocytes [32]. A relatively uniform $I_{to,s}/I_{to,f}$ fraction (between 30 and 40%) supports the notion that a common and tightly regulated molecular mechanism underlies the observed remodeling. In accordance with Kv1.4 up-regulation as the basis for the $I_{to,s}$ emergence when Kv4.2/KChIP2-mediated $I_{to,f}$ is absent [39] Thomsen et al. showed that in KChIP2$^{-/-}$ myocytes a heteropodatoxin-sensitive current component was absent and the 4-aminopyridine-sensitive component was increased [21]. However, their RT-PCR data suggested increased Kv4.2, Kv4.3 and Kv1.5 messages in KChIP2$^{-/-}$ ventricles [21]. By implication, up-regulation of Kv1.5 in KChIP2$^{-/-}$ myocytes would be in accordance with the reported suppression of Kv1.5 on heterologous coexpression with KChIP2 [41]. However, our data do not support $I_{K,slow1}$ up-regulation in KChIP2$^{-/-}$ myocytes of either sex (A2 and D2 in Tables 1 and 2).

The kinetics of recovery from inactivation are usually a good indicator of electrical remodeling. Our results indicate the virtual absence of typical $I_{to,f}$ recovery kinetics (see above) in KChIP2$^{-/-}$ myocytes (see Tables 1 and 2). This probably allows the fast $I_{K,slow1}$ recovery component and/or $I_{K,slow2}$ recovery kinetics (recovery time constants between 350 and 400 ms, [25]) to come to the fore. The second recovery component was also slowed in KChIP2$^{-/-}$ myocytes, probably due to both a shift of $I_{K,slow}$ recovery components into the first component and an up-regulation of the $I_{to,s}$ recovery component (recovery time constant ~ 2000 ms, [25]; see Tables 1 and 2). An intriguing finding of the present study is the modified voltage dependence of inactivation found in KChIP2$^{-/-}$ myocytes. We observed that the more negative component ($V_{1/2}1$) was shifted to even more negative potentials but only accounted for 10–12% (Tables 1 and 2). By implication, a causal relationship between the absence of KChIP2 and the negative shift in $V_{1/2}1$ is supported by the fact that heterologous KChIP2 coexpression shifts the voltage dependence of Kv4 channel inactivation in the positive direction [14]. Thus, the modified inactivation curves of KChIP2$^{-/-}$ myocytes may indicate a small amount of Kv4 channels reaching the cardiomyocyte plasma membrane without the need of KChIP2. This hypothesis is supported by our relA1 values (16% in male and 20% in female KChIP2$^{-/-}$ myocytes; Tables 1 and 2), but not by Foeger et al., who reported the absence of Kv4.2 protein in KChIP2$^{-/-}$ ventricles [31]. A possible coexistence of $I_{to,s}$ and $I_{to,f}$ in the absence of KChIP2 needs further investigation, considering prominent Kv4.3 up-regulation [21, 32] as a candidate mechanism.

Dynamics of functional Kv4.2/KChIP2 expression

Functional expression of Kv4 channels (i.e., subunit assembly, trafficking to the surface membrane and complex stability) is known to be augmented by KChIPs in heterologous expression systems [8, 14, 16–19], but the role of KChIPs in cardiomyocytes has remained undefined for a

long time. In murine ventricular myocytes I_{to} is mainly carried by Kv4.2 channels associated with KChIP2, and targeted deletion of the KChIP2 gene ($KChIP2^{-/-}$) virtually eliminates the Kv4.2 channel-mediated I_{to} [9, 21, 31, 33, 38]. The latter finding alone represents a strong argument for KChIP2 being essential for the functional Kv4.2 expression and thus, being a key regulator of I_{to}. The critical role of KChIP2 in I_{to} expression becomes even more evident by the finding that there is a gene dosage effect, with an intermediate I_{to} magnitude in the heterozygous genotype ($KChIP2^{+/-}$), as reported by Kuo et al. [9]. In order to corroborate this finding, we applied a completely different I_{to} isolation method and compared different KChIP2 genotypes in male and female myocytes. We found a distinct KChIP2 gene dosage effect on I_{to} magnitude in both sexes.

In diploid organisms the presence of two alleles for a gene locus is set to 100%. This percentage can be larger, for instance in trisomies (150%), or 50% if one allele is missing, as in the $KChIP2^{+/-}$ genotype. We asked how strictly a given allelic percentage is converted into a certain phenotype (i.e., amount of protein and eventually protein function). The KChIP2 genotype dependence can be quantified by calculating the relative I_{to} magnitude for $KChIP2^{+/-}$ compared to $KChIP2^{+/+}$. In the present study we obtained heterozygous I_{to} fractions of 63% and 66%, respectively, and heterozygous I_{to} density fractions of 71% and 61%, respectively, for male and female myocytes. Our fractions are larger than the density fraction reported by Kuo et al. (42%; [9]), and also larger than the theoretical value of 50%, assuming a strict conversion of the number of alleles. A possible explanation for this deviation would be the up-regulation of a KChIP2-unrelated I_{to} component (e.g., $I_{to,s}$), not only in $KChIP2^{-/-}$ but also in $KChIP2^{+/-}$ myocytes. In that case one would expect a modulation of inactivation properties. However, we detected no significant differences concerning the inactivation properties of $KChIP2^{+/+}$ and $KChIP2^{+/-}$ myocytes, making an appreciable $I_{to,s}$ up-regulation in $KChIP2^{+/-}$ myocytes unlikely. It should be noted that in female $KChIP2^{+/-}$ myocytes a vague KChIP2 gene dosage effect on inactivation properties was seen (see Fig 7A and 7D). In this context it is intriguing that a number of inactivation parameters, all related to I_{to}, differed between male and female $KChIP2^{+/+}$ myocytes (see Table 2). Some of the observed differences (faster I_{to} decay kinetics and more negative $V_{1/2}1$) create the impression that the KChIP2 effect on inactivation properties has not become fully manifest in female myocytes. However, this does not apply to the kinetics of recovery from inactivation, because $\tau_{rec}1$ was smaller in female than in male myocytes. It has been reported that Kv1.5 and Kv4.3 expression is lower in ventricular myocytes from female mice [28, 42]. Althogh these findings would offer a possible explanation for the different inactivation properties in female myocytes, we detected neither gender-dependent differences in $I_{K,slow}$ densities (in accordance with Brunet et al. [43]) nor a KChIP2 genotype-dependent modulation of $I_{K,slow}$ densities (in contrast to Thomsen et al. [21]). A possible connectivity between the characteristic electrophysiological features and the tentative KChIP2 gene dosage effect on inactivation properties in female myocytes, was not further analyzed.

In the present study the partial KChIP2 gene dosage effect in cardiomyocytes (distinct KChIP2 gene dosage effect on I_{to} magnitude but not on inactivation properties) could be reproduced in a heterologous expression system by injecting a fixed amount of Kv4.2 cRNA with variable amounts of KChIP2 cRNA in *Xenopus* oocytes. The observed increase in the measured current amplitudes with increased amounts of KChIP2 cRNA was expected and most likely due to an increased amount of KChIP2 and increased surface expression of Kv4.2 [19, 44, 45]. Moreover, we show that the KChIP2-dependent gain in current amplitude resembles a logarithmic growth curve, with the typical two portions of steep and shallow increment, respectively (see S3 Fig). It is remarkable that the peak current amplitude of an ion channel correlates so tightly with the cRNA dose of its β-subunit, supporting the notion that KChIP2 is a key regulator of functional Kv4.2 expression. Our results for macroscopic inactivation and

recovery from inactivation of Kv4.2 channels in oocytes were similar to the ones obtained by Goltz et al. with KChIP2 [46] and by Kitazawa et al. with KChIP4 [44]. However, the results of the present study provide clear evidence that the KChIP2 dose dependence of Kv4.2 surface expression differs from the KChIP2 dose dependence of Kv4.2 inactivation gating (see Fig 8F–8H and S3 Fig). Two remarkable findings of our oocyte experiments reflect the partial KChIP2 gene dosage effect: First, current amplitude could be further increased, albeit shallowly, by using KChIP2 cRNA amounts well above saturation for effects on macroscopic inactivation and recovery from inactivation; and secondly, varying the KChIP2 cRNA amount in the steep portion of the logarithmic function curve for peak current amplitude has neglible effects on inactivation gating (see Fig 8 and S3 Fig). Above all, it is intriguing that, by using low amounts of KChIP2 cRNA, the I_{to} inactivation properties seen in KChIP2$^{+/+}$ and KChIP2$^{+/-}$ myocytes could be reproduced (see Fig 8B and 8C). Furthermore, when reducing the KChIP2 cRNA amount by 50% (from 0.4 to 0.2 ng per oocyte or from 0.2 to 0.1 ng per oocyte) the fractional amplitude of oocyte currents is 63% or 69%, respectively. The latter results are directly transferable to our KChIP2 gene dosage effect on I_{to} magnitude in cardiomyocytes (heterozygous I_{to} fractions of 63 and 66%; see above). Our combined results support the notion that in cardiomyocytes a KChIP2 allele number of 50% is not strictly translated into I_{to} magnitude. They imply that the wild-type allele number (100%) provides saturating amounts of KChIP2 to ensure I_{to} expression.

Increasing the KChIP2 cRNA amount well above a value that can reproduce our cardiomyocyte results (e.g., 0.8 ng per oocyte or higher) caused a further slowing of macroscopic inactivation and further acceleration of recovery from inactivation (see Fig 8). Notably, the KChIP2 dose dependence of $\tau_{inact}1$ was smooth and probably reflects the functional stoichiometry of N-type inactivation ([47, 48]; see also S3B Fig). By contrast, $\tau_{inact}2$ and τ_{rec} showed distinct levels, probably reflecting the fact that both $\tau_{inact}2$ and τ_{rec} are merely related to the allosteric mechanism of Kv4.2 closed-state inactivation ([49]; see also S3C and S3D Fig). Our oocyte data raise the question whether in KChIP2$^{+/+}$ myocytes the KChIP2 effects on inactivation properties are at all saturated, which automatically leads to the question regarding the stoichiometry of Kv4.2/KChIP2 complexes in the cardiomyocyte membrane (i.e., how many KChIP2 molecules are bound to a Kv4.2 channel). Based on the analysis of purified channels and crystal structure data it has been commonly thought that Kv4 α-subunits and KChIPs form an octameric complex with a 4:4 stoichiometry [50–53]. However, in these experimental approaches KChIP was present in excess. More recently, Kitazawa and coworkers found that both the biophysical properties and the stoichiometry of Kv4.2/KChIP4 channels depend critically on the amount of KChIP4 coexpressed in *Xenopus* oocytes [44]. The authors concluded that Kv4.2/KChIP4 channel complexes may have variable stoichiometries depending on the amount of KChIP4 available, and that stoichiometry dictates channel gating. Both Kv4 and KChIP expression are developmentally regulated [54–57], such that their relative amounts and the Kv4/KChIP stoichiometry and, thus I_{to} properties, may change with age. Kv4 and KChIP expression are even regulated based on a circadian rhythm [58, 59], which may allow a more short-term regulation of I_{to} properties. Whether KChIP molecules freely moving in the cytosol [19, 44] are available for spontaneous binding to Kv4.2 channels in the plasma membrane, thereby allowing a most acute form of I_{to} regulation, remains to be examined.

In summary, our results support the notion that cardiomyocytes normally produce enough KChIP2 to ensure I_{to} expression. On the other hand, the molecular correlate of I_{to} seems to be highly dynamic, such that changes in the amount of KChIP2 may create a considerable scope concerning I_{to} properties in remodeling processes including cardiac memory, hypertrophy and heart failure [60].

Supporting information

S1 Fig. Prepulse-inactivation-subtraction method applied to male cardiomyocytes with different KChIP2 genotypes. Individual myocytes were isolated from the left ventricular free wall of male mice and currents were measured with the whole-cell patch-clamp technique. The voltage protocol used for the prepulse-inactivation-subtraction method is depicted on the lower right (D). Compound outward currents (1) were activated by a voltage pulse from -80 to +40 mV. Sodium currents (not recorded at their full size) were inactivated by a brief (8 ms) prepulse to -50 mV. A fraction of outward current was inactivated by a 160 ms prepulse to -40 mV (2). Subtraction of 1–2 yielded a rapidly decaying current trace referred to as I_{to}. The decay of this current trace was fitted by a single-exponential function (red). Application of this method is shown for a KChIP2$^{+/+}$ (A) and a KChIP2$^{+/-}$ myocyte (B) and two KChIP2$^{-/-}$ myocytes (C and D). In some KChIP2$^{-/-}$ myocytes the method yielded current traces with extremely small amplitudes (i.e., I_{to} was virtually lost), however, the time course of current decay could still be fitted by a single-exponential function (C).
(PDF)

S2 Fig. Expression profiles of Kv4.2 and Kv4.2/KChIP2 channels in *Xenopus* oocytes. Oocytes were surgically removed and treated with collagenase. Predefined amounts of Kv4.2 and KChIP2 cRNA were injected into individual oocytes, and currents were measured with the two-electrode voltage-clamp technique. A. Functional expression of Kv4.2 and Kv4.2/KChIP2 channels over time. Oocytes were injected with 1 ng Kv4.2 cRNA alone or coinjected with 1 ng Kv4.2 and 1 ng KChIP2 cRNA. Peak current amplitudes were measured 24, 48, 72 and 96 h after cRNA injection. B. For each time of recording the fold gain in peak current amplitude in the presence of KChIP2 compared to Kv4.2 alone was determined.
(PDF)

S3 Fig. Dependence of Kv4.2 properties on the amount of coinjected KChIP2 cRNA. A fixed amount of 1 ng Kv4.2 cRNA was coinjected with different amounts of KChIP2 cRNA (0, 0.1, 0.2, 0.4, 0.8, 1.6, 3.2, 6.4 and 12.8 ng) into individual oocytes, and currents were recorded 48 h after cRNA injection. Various current parameters were analyzed, and the results were plotted against the amount of coinjected KChIP2 cRNA. A. Peak current amplitude; a logarithmic fit represents a good description of the data, indicating that a steeper portion of the function (low to intermediate KChIP2 cRNA amounts, $y < 19$ μA) can be distinguished from a shallower portion (high KChIP2 cRNA amounts, $y > 19$ μA). The KChIP2 cRNA amounts of 0.4 and 0.2 ng per oocyte lie within the steep portion and the relative difference in amplitude is 63%, very similar to the relative differences between the I_{to} amplitudes obtained for KChIP2$^{+/+}$ and KChIP2$^{+/-}$, respectively, in both male (63%) and female cardiomyocytes (66%). B. First inactivation time constant ($\tau_{inact}1$) obtained with a double-exponential fit to the current decay; a logarithmic function describes the data well for low to intermediate KChIP2 cRNA amounts ($y \leq 56$ ms). However, at higher KChIP2 cRNA amounts $\tau_{inact}1$ saturates at ~ 80 ms. C. Second inactivation time constant ($\tau_{inact}2$) obtained with a double-exponential fit to the current decay; a logarithmic function does not describe the data very well. The mean $\tau_{inact}2$ is ~ 200 ms in the absence of KChIP2, between 400 and 600 ms at low to intermediate amounts and ~ 1000 ms at high amounts of KChIP2 cRNA. D. Recovery time constant (τ_{rec}). Similar to $\tau_{inact}2$, the recovery data cannot be well described by a logarithmic function. The mean τ_{rec} is ~ 700 ms in the absence of KChIP2, between 150 and 250 ms at low to intermediate KChIP2 cRNA amounts and ~ 40 ms at KChIP2 cRNA amounts of 0.8 ng per oocyte and higher.
(PDF)

S1 Table. Data summary for the prepulse-inactivation-subtraction method applied to male cardiomyocytes.
(PDF)

Acknowledgments

We thank Kenneth Chien for the permission to use his KChIP2 knockout model, Morton B. Thomsen for helping to initialize the corresponding mouse line in our institution, Telse Kock and Margrit Hölzel for genotyping murine tissues and cRNA synthesis and Susanne Lezius for advice on statistical analyses.

Author Contributions

Conceptualization: RB.

Data curation: LW VJ RB.

Formal analysis: LW VJ RB.

Funding acquisition: RB.

Investigation: LW VJ RB.

Methodology: LW VJ.

Project administration: RB.

Supervision: RB.

Validation: RB.

Visualization: LW VJ RB.

Writing – original draft: RB.

Writing – review & editing: RB LW VJ.

References

1. Nerbonne JM, Kass RS. Molecular physiology of cardiac repolarization. Physiological reviews. 2005; 85:1205–53. doi: 10.1152/physrev.00002.2005 PMID: 16183911
2. Sah R, Ramirez RJ, Oudit GY, Gidrewicz D, Trivieri MG, Zobel C, et al. Regulation of cardiac excitation-contraction coupling by action potential repolarization: Role of the transient outward potassium current (I_{to}). The journal of physiology. 2003; 546:5–18. doi: 10.1113/jphysiol.2002.026468 PMID: 12509475
3. Barry DM, Xu H, Schuessler RB, Nerbonne JM. Functional knockout of the transient outward current, long-QT syndrome, and cardiac remodeling in mice expressing a dominant-negative Kv4 α subunit. Circulation research. 1998; 83:560–7. PMID: 9734479
4. Dixon JE, Shi W, Wang HS, McDonald C, Yu H, Wymore RS, et al. Role of the Kv4.3 K^+ channel in ventricular muscle. A molecular correlate for the transient outward current. Circulation research. 1996; 79:659–68. PMID: 8831489
5. Fiset C, Clark RB, Shimoni Y, Giles WR. Shal-type channels contribute to the Ca^{2+}-independent transient outward K^+ current in rat ventricle. The Journal of physiology. 1997; 500:51–64. PMID: 9097932
6. Guo W, Li H, Aimond F, Johns DC, Rhodes KJ, Trimmer JS, et al. Role of heteromultimers in the generation of myocardial transient outward K^+ currents. Circulation research. 2002; 90:586–93. PMID: 11909823
7. Johns DC, Nuss HB, Marban E. Suppression of neuronal and cardiac transient outward currents by viral gene transfer of dominant-negative Kv4.2 constructs. The Journal of biological chemistry. 1997; 272:31598–603. PMID: 9395498

8. An WF, Bowlby MR, Betty M, Cao J, Ling HP, Mendoza G, et al. Modulation of A-type potassium channels by a family of calcium sensors. Nature. 2000; 403:553–6. doi: 10.1038/35000592 PMID: 10676964
9. Kuo HC, Cheng CF, Clark RB, Lin JJ, Lin JL, Hoshijima M, et al. A defect in the Kv Channel-Interacting Protein 2 (KChIP2) gene leads to a complete loss of I_{to} and confers susceptibility to ventricular tachycardia. Cell. 2001; 107:801–13. PMID: 11747815
10. Isbrandt D, Leicher T, Waldschütz R, Zhu X, Luhmann U, Michel U, et al. Gene structures and expression profiles of three human KCND (Kv4) potassium channels mediating A-type currents I_{TO} and I_{SA}. Genomics. 2000; 64:144–54. doi: 10.1006/geno.2000.6117 PMID: 10729221
11. Decher N, Barth AS, Gonzalez T, Steinmeyer K, Sanguinetti MC. Novel KChIP2 isoforms increase functional diversity of transient outward potassium currents. The Journal of physiology. 2004; 557:761–72. doi: 10.1113/jphysiol.2004.066720 PMID: 15107477
12. Pruunsild P, Timmusk T. Structure, alternative splicing, and expression of the human and mouse KCNIP gene family. Genomics. 2005; 86:581–93. doi: 10.1016/j.ygeno.2005.07.001 PMID: 16112838
13. Patel SP, Campbell DL. Transient outward potassium current, 'I_{to}', phenotypes in the mammalian left ventricle: underlying molecular, cellular and biophysical mechanisms. The Journal of physiology. 2005; 569:7–39. doi: 10.1113/jphysiol.2005.086223 PMID: 15831535
14. Bähring R, Dannenberg J, Peters HC, Leicher T, Pongs O, Isbrandt D. Conserved Kv4 N-terminal domain critical for effects of Kv channel-interacting protein 2.2 on channel expression and gating. The Journal of biological chemistry. 2001; 276:23888–94. doi: 10.1074/jbc.M101320200 PMID: 11287421
15. Beck EJ, Bowlby M, An WF, Rhodes KJ, Covarrubias M. Remodelling inactivation gating of Kv4 channels by KChIP1, a small-molecular-weight calcium-binding protein. The Journal of physiology. 2002; 538:691–706. doi: 10.1113/jphysiol.2001.013127 PMID: 11826158
16. Foeger NC, Marionneau C, Nerbonne JM. Co-assembly of Kv4 α subunits with K^+ channel-interacting protein 2 stabilizes protein expression and promotes surface retention of channel complexes. The Journal of biological chemistry. 2010; 285:33413–22. doi: 10.1074/jbc.M110.145185 PMID: 20709747
17. Hasdemir B, Fitzgerald DJ, Prior IA, Tepikin AV, Burgoyne RD. Traffic of Kv4 K^+ channels mediated by KChIP1 is via a novel post-ER vesicular pathway. The Journal of cell biology. 2005; 171:459–69. doi: 10.1083/jcb.200506005 PMID: 16260497
18. Kunjilwar K, Strang C, DeRubeis D, Pfaffinger PJ. KChIP3 rescues the functional expression of Shal channel tetramerization mutants. The Journal of biological chemistry. 2004; 279:54542–51. doi: 10.1074/jbc.M409721200 PMID: 15485870
19. Shibata R, Misonou H, Campomanes CR, Anderson AE, Schrader LA, Doliveira LC, et al. A fundamental role for KChIPs in determining the molecular properties and trafficking of Kv4.2 potassium channels. The Journal of biological chemistry. 2003; 278:36445–54. doi: 10.1074/jbc.M306142200 PMID: 12829703
20. Rosati B, Pan Z, Lypen S, Wang HS, Cohen I, Dixon JE, et al. Regulation of KChIP2 potassium channel β subunit gene expression underlies the gradient of transient outward current in canine and human ventricle. The Journal of physiology. 2001; 533:119–25. doi: 10.1111/j.1469-7793.2001.0119b.x PMID: 11351020
21. Thomsen MB, Sosunov EA, Anyukhovsky EP, Özgen N, Boyden PA, Rosen MR. Deleting the accessory subunit KChIP2 results in loss of $I_{to,f}$ and increased $I_{K,slow}$ that maintains normal action potential configuration. Heart Rhythm. 2009; 6:370–7. doi: 10.1016/j.hrthm.2008.11.023 PMID: 19251214
22. Guénette SA, Giroux MC, Vachon P. Pain perception and anaesthesia in research frogs. Experimental animals. 2013; 62:87–92. PMID: 23615302
23. Brouillette J, Clark RB, Giles WR, Fiset C. Functional properties of K^+ currents in adult mouse ventricular myocytes. The Journal of physiology. 2004; 559:777–98. doi: 10.1113/jphysiol.2004.063446 PMID: 15272047
24. Guo W, Xu H, London B, Nerbonne JM. Molecular basis of transient outward K^+ current diversity in mouse ventricular myocytes. The Journal of physiology. 1999; 521:587–99. doi: 10.1111/j.1469-7793.1999.00587.x PMID: 10601491
25. Liu J, Kim KH, London B, Morales MJ, Backx PH. Dissection of the voltage-activated potassium outward currents in adult mouse ventricular myocytes: $I_{to,f}$, $I_{to,s}$, $I_{K,slow1}$, $I_{K,slow2}$, and I_{ss}. Basic research in cardiology. 2011; 106:189–204. doi: 10.1007/s00395-010-0134-z PMID: 21253754
26. Xu H, Guo W, Nerbonne JM. Four kinetically distinct depolarization-activated K^+ currents in adult mouse ventricular myocytes. The Journal of general physiology. 1999; 113:661–78. PMID: 10228181
27. Tozakidou M, Goltz D, Hagenström T, Budack MK, Vitzthum H, Szlachta K, et al. Molecular and functional remodeling of I_{to} by angiotensin II in the mouse left ventricle. Journal of molecular and cellular cardiology. 2010; 48:140–51. doi: 10.1016/j.yjmcc.2009.08.027 PMID: 19744491

28. Trépanier-Boulay V, St-Michel C, Tremblay A, Fiset C. Gender-based differences in cardiac repolarization in mouse ventricle. Circulation research. 2001; 89:437–44. PMID: 11532905

29. Clark RB, Tremblay A, Melnyk P, Allen BG, Giles WR, Fiset C. T-tubule localization of the inward-rectifier K^+ channel in mouse ventricular myocytes: a role in K^+ accumulation. The Journal of physiology. 2001; 537:979–92. doi: 10.1111/j.1469-7793.2001.00979.x PMID: 11744770

30. Costantini DL, Arruda EP, Agarwal P, Kim KH, Zhu Y, Zhu W, et al. The homeodomain transcription factor Irx5 establishes the mouse cardiac ventricular repolarization gradient. Cell. 2005; 123:347–58. doi: 10.1016/j.cell.2005.08.004 PMID: 16239150

31. Foeger NC, Wang W, Mellor RL, Nerbonne JM. Stabilization of Kv4 Protein by the accessory K^+ Channel Interacting Protein 2 (KChIP2) subunit is required for the generation of native myocardial fast transient outward K^+ currents. The Journal of physiology. 2013; 591:4149–66. doi: 10.1113/jphysiol.2013.255836 PMID: 23713033

32. Liu J, Kim KH, Morales MJ, Heximer SP, Hui CC, Backx PH. Kv4.3-encoded fast transient outward current is presented in Kv4.2 knockout mouse cardiomyocytes. PLOS ONE. 2015; 10:e0133274. doi: 10.1371/journal.pone.0133274 PMID: 26196737

33. Niwa N, Wang W, Sha Q, Marionneau C, Nerbonne JM. Kv4.3 is not required for the generation of functional $I_{to,f}$ channels in adult mouse ventricles. Journal of molecular and cellular cardiology. 2008; 44:95–104. doi: 10.1016/j.yjmcc.2007.10.007 PMID: 18045613

34. Wang L, Duff HJ. Developmental changes in transient outward current in mouse ventricle. Circulation research. 1997; 81:120–7. PMID: 9201035

35. Niwa N, Nerbonne JM. Molecular determinants of cardiac transient outward potassium current (I_{to}) expression and regulation. Journal of molecular and cellular cardiology. 2010; 48:12–25. doi: 10.1016/j.yjmcc.2009.07.013 PMID: 19619557

36. London B, Wang DW, Hill JA, Bennett PB. The transient outward current in mice lacking the potassium channel gene Kv1.4. The Journal of physiology. 1998; 509:171–82. doi: 10.1111/j.1469-7793.1998.171bo.x PMID: 9547391

37. Wickenden AD, Lee P, Sah R, Huang Q, Fishman GI, Backx PH. Targeted expression of a dominant-negative Kv4.2 K^+ channel subunit in the mouse heart. Circulation research. 1999; 85:1067–76. PMID: 10571538

38. Guo W, Jung WE, Marionneau C, Aimond F, Xu H, Yamada KA, et al. Targeted deletion of Kv4.2 eliminates $I_{to,f}$ and results in electrical and molecular remodeling, with no evidence of ventricular hypertrophy or myocardial dysfunction. Circulation research. 2005; 97:1342–50. doi: 10.1161/01.RES.0000196559.63223.aa PMID: 16293790

39. Guo W, Li H, London B, Nerbonne JM. Functional consequences of elimination of $I_{to,f}$ and $I_{to,s}$: early afterdepolarizations, atrioventricular block, and ventricular arrhythmias in mice lacking Kv1.4 and expressing a dominant-negative Kv4 α subunit. Circulation research. 2000; 87:73–9. PMID: 10884375

40. Grubb S, Speerschneider T, Occhipinti D, Fiset C, Olesen SP, Thomsen MB, et al. Loss of K^+ currents in heart failure is accentuated in KChIP2 deficient mice. Journal of cardiovascular electrophysiology. 2014; 25:896–904. doi: 10.1111/jce.12422 PMID: 24678923

41. Li H, Guo W, Mellor RL, Nerbonne JM. KChIP2 modulates the cell surface expression of Kv 1.5-encoded K^+ channels. Journal of Molecular and cellular cardiology. 2005; 39:121–32. doi: 10.1016/j.yjmcc.2005.03.013 PMID: 15878168

42. Saito T, Ciobotaru A, Bopassa JC, Toro L, Stefani E, Eghbali M. Estrogen contributes to gender differences in mouse ventricular repolarization. Circulation research. 2009; 105:343–52. doi: 10.1161/CIRCRESAHA.108.190041 PMID: 19608983

43. Brunet S, Aimond F, Li H, Guo W, Eldstrom J, Fedida D, et al. Heterogeneous expression of repolarizing, voltage-gated K^+ currents in adult mouse ventricles. The Journal of physiology. 2004; 559:103–20. doi: 10.1113/jphysiol.2004.063347 PMID: 15194740

44. Kitazawa M, Kubo Y, Nakajo K. The stoichiometry and biophysical properties of the Kv4 potassium channel complex with K^+ channel-interacting protein (KChIP) subunits are variable, depending on the relative expression level. The Journal of biological chemistry. 2014; 289:17597–609. doi: 10.1074/jbc.M114.563452 PMID: 24811166

45. Rosati B, Grau F, Rodriguez S, Li H, Nerbonne JM, McKinnon D. Concordant expression of KChIP2 mRNA, protein and transient outward current throughout the canine ventricle. The Journal of physiology. 2003; 548:815–22. doi: 10.1113/jphysiol.2002.033704 PMID: 12598586

46. Goltz D, Schultz JH, Stucke C, Wagner M, Bassalay P, Schwoerer AP, et al. Diminished Kv4.2/3 but not KChIP2 levels reduce the cardiac transient outward K^+ current in spontaneously hypertensive rats. Cardiovascular research. 2007; 74:85–95. doi: 10.1016/j.cardiores.2007.01.001 PMID: 17289007

47. Gebauer M, Isbrandt D, Sauter K, Callsen B, Nolting A, Pongs O, et al. N-type inactivation features of Kv4.2 channel gating. Biophysical journal. 2004; 86:210–23. doi: 10.1016/S0006-3495(04)74097-7 PMID: 14695263

48. MacKinnon R, Aldrich RW, Lee AW. Functional stoichiometry of Shaker potassium channel inactivation. Science. 1993; 262:757–9. PMID: 7694359

49. Bähring R, Covarrubias M. Mechanisms of closed-state inactivation in voltage-gated ion channels. The Journal of physiology. 2011; 589:461–79. doi: 10.1113/jphysiol.2010.191965 PMID: 21098008

50. Kim LA, Furst J, Butler MH, Xu S, Grigorieff N, Goldstein SA. I_{to} channels are octomeric complexes with four subunits of each Kv4.2 and K^+ channel-interacting protein 2. The Journal of biological chemistry. 2004; 279:5549–54. doi: 10.1074/jbc.M311332200 PMID: 14623880

51. Kim LA, Furst J, Gutierrez D, Butler MH, Xu S, Goldstein SA, et al. Three-dimensional structure of I_{to}; Kv4.2-KChIP2 ion channels by electron microscopy at 21 Å resolution. Neuron. 2004; 41:513–9. PMID: 14980201

52. Pioletti M, Findeisen F, Hura GL, Minor DL Jr. Three-dimensional structure of the KChIP1-Kv4.3 T1 complex reveals a cross-shaped octamer. Nature structural and molecular biology. 2006; 13:987–95. doi: 10.1038/nsmb1164 PMID: 17057713

53. Wang H, Yan Y, Liu Q, Huang Y, Shen Y, Chen L, et al. Structural basis for modulation of Kv4 K^+ channels by auxiliary KChIP subunits. Nature neuroscience. 2007; 10:32–9. doi: 10.1038/nn1822 PMID: 17187064

54. Gönczi M, Birinyi P, Balázs B, Szentandrássy N, Harmati G, Könczei Z, et al. Age-dependent changes in ion channel mRNA expression in canine cardiac tissues. General physiology and biophysics. 2012; 31:153–62. doi: 10.4149/gpb_2012_017 PMID: 22781818

55. Kobayashi T, Yamada Y, Nagashima M, Seki S, Tsutsuura M, Ito Y, et al. Contribution of KChIP2 to the developmental increase in transient outward current of rat cardiomyocytes. Journal of molecular and cellular cardiology. 2003; 35:1073–82. PMID: 12967630

56. Plotnikov AN, Sosunov EA, Patberg KW, Anyukhovsky EP, Gainullin RZ, Shlapakova IN, et al. Cardiac memory evolves with age in association with development of the transient outward current. Circulation. 2004; 110:489–95. doi: 10.1161/01.CIR.0000137823.64947.52 PMID: 15262840

57. Wang Y, Xu H, Kumar R, Tipparaju SM, Wagner MB, Joyner RW. Differences in transient outward current properties between neonatal and adult human atrial myocytes. Journal of molecular and cellular cardiology. 2003; 35:1083–92. PMID: 12967631

58. Jeyaraj D, Haldar SM, Wan X, McCauley MD, Ripperger JA, Hu K, et al. Circadian rhythms govern cardiac repolarization and arrhythmogenesis. Nature. 2012; 483:96–9. doi: 10.1038/nature10852 PMID: 22367544

59. Yamashita T, Sekiguchi A, Iwasaki YK, Sagara K, Iinuma H, Hatano S, et al. Circadian variation of cardiac K^+ channel gene expression. Circulation. 2003; 107:1917–22. doi: 10.1161/01.CIR.0000058752.79734.F0 PMID: 12668525

60. Grubb S, Calloe K, Thomsen MB. Impact of KChIP2 on cardiac electrophysiology and the progression of heart failure. Frontiers in physiology. 2012; 3:118. doi: 10.3389/fphys.2012.00118 PMID: 22586403